
Marco Gonzalez, Ambergris Caye, Belize: A geoarchaeological record of ground raising associated with surface soil formation and the presence of a Dark Earth

By

Richard. I. Macphail¹, Elizabeth Graham¹, John Crowther² and Simon Turner³

1: University College London, Institute of Archaeology, 31-34, Gordon Sq., London WC1H 0PY, UK,; 2: Archaeological Services, Trinity St Davids, University of Wales, Lampeter, Ceredigion, UK SA48 7ED, UK, ; 3: University College London, Environmental Change Research Centre, Gower Street, London WC1E 6BT, UK

Corresponding author:

Email address: r.macphail@ucl.ac.uk (R. Macphail), e.graham@ucl.ac.uk (E. Graham), simon.turner@ucl.ac.uk (S. Turner)

Keywords:

Maya

Soil micromorphology

Chemistry

Floors

Salt working

Dark Earth

Mercury

Highlights

- Maya site formation processes including ground-raising from industrial activity and waste accumulation.
- Insights into off site mud flat sedimentation from sponge spicule-rich clays used as a lime plaster floor temper and as a hypothetical source for producing brine for salt processing.
- Late Classic marine inundation event at ca. 0.39m asl.
- The characterisation of a Maya Dark Earth formed from weathered lime floors and ash deposits in contrast to typical Amazonian Dark Earths.
- A proposal to distinguish modern surface soils from a Dark Earth owing to the paucity of charcoal and the presence of elements such as mercury.

Abstract

Marco Gonzalez, on the south-west end of the island of Ambergris Caye, Belize, has well-preserved Maya archaeological stratigraphy dating from Preclassic times (ca. 300 B.C.) to the

Late Classic period (ca. A.D. 550/600 to 700/760). Although later occupations are recorded by house platforms and inhumations (Terminal Classic to Early Postclassic), and use of the site continued until the 16th century A.D., intact stratigraphy is rare in these cases owing to a greater degree of disturbance. Nonetheless, understanding site formation entails accounting for all processes, including disturbance. The site's depositional sequence—as revealed through soil micromorphology and chemistry and detailed here—has yielded critical information in two spheres of research. As regards archaeology and the elucidation of Maya activities on the caye over time, soil micromorphology has contributed beyond measure to what we have been able to distinguish as material remains of cultural activity. Detailed descriptions of the nature of the material remains has in turn helped us to clarify or alter interpretations based on artefacts that have been identified or sediments characterised according to traditional recovery techniques. The other major sphere in which soil micromorphology and chemistry play a critical role is in assessment of the environmental impact of human activity, which enables us to construct and test hypotheses concerning how the site formed over time; what materials and elements contributed to the character of the sediments, especially in the formation of a specific Maya Dark Earth type that is developed from carbonate rich deposits; and how the modern surface soils acquired the appearance of a Dark Earth, but essentially differ from them. In terms of agricultural soil sustainability, the Marco Gonzalez topsoil is neo-formed by a woodland vegetation drawing upon the nutrients present in the Dark Earth and underlying better preserved stratified deposits.

1. Introduction

A multi-disciplinary study of selected geoarchaeological and archaeological sequences was carried out at the Maya site of Marco Gonzalez, Ambergris Caye, Belize during 2013-2014 to investigate site formation processes. Understanding site formation is only one of a set of aims whose common properties are defined by our goal of elucidating the long-term role of human impact in the formation of the earth's cultivable soils (Graham et al. 2015). The content of this paper in particular is focused on describing the methods that we employed to sample, describe, analyse, and interpret all of the accessible strata that comprise the archaeological site. Our hope is that such methods—duplicated, altered, or improved—will be of utility to other researchers. Before describing the methods and results of the site formation research, and in order to contextualise the data and discussion presented here, we provide an outline of the cultural context and anthropological significance of the larger study,

otherwise detailed extensively in other publications (Graham 1992, 1998, 2006; Graham et al. 2015).

2015).

2. Site formation and its significance

One aim of characterising site formation processes, which is perhaps the original aim in archaeology, has been to contribute to a better understanding of the contexts for

archaeological evidence (Schiffer 1987). Soil micromorphological approaches have contributed inestimably to this aim at Marco Gonzalez. The results of soil micromorphological analyses have strengthened our hypothesis that salt production was an intensive economic activity at Marco Gonzalez in the Late Classic period (ca. A.D. 550 to 750). There are other instances, however, in which micromorphology has provided information on the origins of sediments that have yielded archaeological material, such as the Terminal Preclassic and Early Classic pottery in colluvial deposits sealed either by subsequent construction or by the debris of salt processing. Information on the material comprising the archaeological deposits—such as the ghost floors in the salt-processing debris and later habitation levels or the coprolitic bone material in the Early Classic levels—was simply not detectable by the naked eye during excavation. It should be noted that the soil micromorphological results, limited thus far to strata exposed in test pits, remain preliminary and much more extensive exposure will be required to gather evidence on the full range of occupational and processing activities at the site. However, the results described should nonetheless serve to demonstrate the ways in which our picture of the activities at the site has been clarified and enriched, and has helped us to develop a strategy for future research.

The other critical role of soil micromorphology is its contribution to our greater goal of assessing the environmental impact of human activity at Marco Gonzalez, which will enable us to construct and test hypotheses concerning how the site formed over time, what materials and elements contributed to the character of the sediments, and how the modern surface soils acquired the appearance of a Dark Earth (Graham et al. 2015). The dark brown to black surface soils, commonly removed by locals for use in their gardens, are typical of sites on the caye and of other sites in coastal Belize (Graham 1994, 2006). They are shown, through the soil micromorphological analyses presented below, to be distinct from Amazonian Dark Earths (ADEs or *terra preta*) (Arroyo-Kalin 2009, 2014; Arroyo-Kalin et al. 2009; Glaser and Birk 2012; Glaser and Woods 2004; Lehman et al. 2003; Sombroek 1966; Woods et al. 2009), but they share critical characteristics, such as the ubiquitous presence of charcoal. Perhaps more important, Maya Dark Earth, like ADE, represents enrichment by activities for which humans were the catalyst. Dark earths have not received much attention in the Maya area, probably owing to the fact that evidence of the kind of enrichment documented for ADEs has been rare (Beach et al. 2015: 18). An initial study of soils at Marco Gonzalez (Beach et al. 2009) has, however, revealed a significant degree of enrichment, which supports

the contention that studies of anthropogenic soils of Precolumbian origin should extend to areas of the Neotropics outside the Amazon (Arroyo-Kalin, 2014: 174; Graham, 2006).

We were able to build on an existing framework of the site's history, the result of excavations carried out in 1986, 1990 and 2010 (Graham and Pendergast, 1989; Graham and Simmons, 2012; Pendergast and Graham, 1987) (Fig 1). Our goal was to determine whether the sub-surface strata reflecting these sequences had contributed to the character of present-day soils and vegetation and, if so, to assess the nature of their contribution. Of major interest are the dark surface soils that are seemingly atypical compared to other Neotropical *terra preta* soils, known as Amazonian Dark Earths or ADEs (Arroyo-Kalin, 2014; Arroyo-Kalin et al., 2008; Graham, 2006). Accumulated remains of Maya occupation (mainly since ca. A.D. 100) including charcoal, pottery, and debris from hypothesised salt processing (A.D. 550/600 to 700/760) were investigated in detail. Development of the coast line, sea level change, mangrove formation, the modern day vegetation (Fig 2), plant macrofossils, the site in its wider landscape and the results of Maya waste disposal in relationship to modern sustainable land use in the region were considered in addition to the geoarchaeological study presented here (Graham *et al.*, 2015). This paper focuses on findings from the salt working levels, on the formation of a Maya Dark Earth, and on current surface soil development.

The island of Ambergris Caye is underlain by 'reefstone' (maximum elevation 1m asl) of the Belize Barrier Reef, which formed >8.26 to 6.68 ky BP on Pleistocene reef limestones (Gischler and Hudson, 2004). Sea level rise since the Pleistocene has affected coastal morphology, with the shelf lagoon between the Belize Barrier Reef and the mainland already inundated by 5.6 ky BP; subsidence associated with fault-blocks below the reef has also occurred (Dunn and Mazzullo, 1993; Gischler and Hudson, 2004, 232-234; Gischler et al., 2000; James and Ginsburg, 1979). The site of Marco Gonzalez with its distinctive vegetation is easily spotted from the air at the southern end of the caye (Figure 2). At 3.5m asl, it appears as a large mound surrounded by mangrove swamp and separated from the windward shores by beach sands. Research by Dunn and Mazzullo (1993) has shown that the site in the past was open to both the Caribbean and to the waters of the lagoon on the leeward side of the island. Preclassic deposits lie largely below the modern water table, but a sample of ceramics recovered from submerged strata indicate occupation at least by Late Preclassic times (ca. 300 BC- A.D.1), with intensification of marine resource exploitation and trading activity during the Terminal Preclassic period (ca. A.D. 1-250). Utilization of the site continued in various forms until early Spanish colonial times. The period that seems to have given the site the bulk of its modern configuration spans the end of the Late Classic to the Early Postclassic (ca. A.D. 760 to 1200). At the end of the Late Classic, sometime in the latter part of the 8th

century A.D., a town of over 40 structures—reefstone platforms with perishable superstructures—was built. It is these structures that were mapped (Figure 3) and provide the loci for the excavation designations (e.g., Str. 1, Str. 22, etc.).

Our study sampled three locations: Str. 14 (Op 13-1), Str. 19 (Op 13-2) and Str. 8 (Op 13-3). The locations of Strs. 14 and 19 represent the highest elevations on site whereas Str. 8 lies at the (present-day) site periphery (Figure 3). No basal boundary between natural sediments and anthropogenic deposits was observed in thin-section samples (lowest sample at -0.23m asl) because the earliest deposits lie below current high groundwater levels and were inaccessible. Earlier stratigraphic surveys by Dunn and Mazullo (1993) propose that anthrosols sit, unconformably on a high shelf of Pleistocene limestone, which may preclude natural sediment being found at greater depth beneath the central area. Occupation detritus (sherds and conch) mixed with open marine sandy carbonate muds, estuarine mud/sand and mangrove sediments were found in cores to the south of the site in 2013. Artefact-containing sands and muds (extending >1.5m below sea level) were recorded at the mangrove site margin (Graham et al., 2015), which suggests that a preserved boundary between natural sediments and earliest anthropogenic deposits can be found at selected locations.

2. Methods

Soil micromorphology focused on continuous and semi-continuous sequences and lateral control samples from the excavation units. Sampling extended from the excavated exposed ‘surface’ or modern topsoil, down to water-saturated levels at Structure 14, for example (-0.230 – 2.150m asl); in addition, three further surface soil locations were studied in thin section at Strs. 8, 19 and 25 (Fig 3). All monoliths (sampling vertical sections through excavated profiles) from Structures 8, 14 and 19 were sub-sampled for a suite of bulk analytical chemical, geophysical and particle-size techniques that had proven useful during investigations of intertidal, coastal salt making and European dark earth sites; European dark earth site-studies are thought to be relevant given the similar amount of lime-based plasters and limestone employed at Marco Gonzalez in comparison to Roman urban sites (Boorman et al., 2002; Borderie et al., 2014; Macphail, 2003; Macphail et al., 2010; Macphail et al., 2012). A parallel series of bulk samples also underwent XRF and Hg analysis. The combined methods were selected to be consistent with those employed studying other Maya sites and Amazonian Dark Earths in general (Arroyo-Kalin, 2014; Arroyo-Kalin et al., 2008; Beach et al., 2006; Beach and Dunning, 1995).

Monoliths were examined and sub-sampled at the Institute of Archaeology, University College London by R. Macphail, so that selected bulk samples exactly matched thin section samples (online Table 1). Bulk soil analyses were carried out by J. Crowther at Trinity St David's, University of Wales, Lampeter; the same sample series underwent XRF and Hg analysis at the Department of Geography, UCL, by Simon Turner. All samples were freeze-dried, sieved at <125 micron and homogenised for measurement of Hg and XRF analysis.

Subsampling for bulk samples and resin-impregnation of intact monolith material for thin section production followed established protocols (Goldberg and Macphail, 2006). Bulk analyses involved the testing of 39 samples for organic matter (LOI: loss-on-ignition), carbonate (LOI @ 950°C), fractionated P, pH, specific conductance ('salinity') and magnetic susceptibility (χ , χ_{\max} and $\% \chi_{\text{conv}}$), with 10 samples also being analysed for particle size (Avery and Bascomb, 1974; Scollar et al., 1990; Tite, 1972; Tite and Mullins, 1971). LOI (organic matter) and carbonate content were determined by sequential ignition: at 375°C for 16 hrs (Ball, 1964) – previous experimental studies having shown that there is normally no significant breakdown of carbonate at this temperature – and at 950°C for 2 hours; for a separate surface soil mapping study carried out at UCL a temperature of 550°C for 2 hours was employed (Heiri et al., 2001). Phosphate-Pi (inorganic phosphate) and phosphate-Po (organic phosphate) were determined using a two-stage adaptation of the procedure developed by Dick and Tabatabai (1977) in which the phosphate concentration of a sample is measured first without oxidation of organic matter (Pi), using 1N HCl as the extractant; and then on the residue following alkaline oxidation with sodium hypobromite (Po), using 1N H₂SO₄ as the extractant. Phosphate-P (total phosphate) has been derived as the sum of phosphate-Pi and phosphate-Po, and the percentages of inorganic and organic phosphate calculated (i.e. phosphate-Pi:P and phosphate-Po:P, respectively). Mercury (Hg) analyses employed cold vapour-atomic fluorescence spectrometry (CV-AFS) at UCL.

Out of a total of 44 thin-sections studied, SEM/EDS (Energy Dispersive X-Ray Spectrometry; Weiner, 2010) was carried out on specific features in 7 thin sections. Thin sections were described, ascribed soil microfabric types (MFTs) and microfacies types (MFTs), and counted according to established methods (Bullock et al., 1985; Courty, 2001; Courty et al., 1989; Macphail and Cruise, 2001; Stoops, 2003; Stoops et al., 2010).

3. Results and preliminary discussion

Results are presented online in Tables 2-5 and illustrated in various thin-section scans, photomicrographs and a SEM X-Ray backscatter example. Presentation of our overall

methodology and its effectiveness in light of preliminary results has been published (Graham et al., 2015). The following sections assess our understanding of deposit accumulation and its significance in relationship to Dark Earth and surface soil formation (Table 1).

Preliminary results from surface soils and off-site sediment sequences

Subsamples from the micromorphology sections show that there is a strong association of Hg with surface humic horizons, compared to units found at depth. Other metals (Ni, Cu, Zn and Pb; Table 2) often associated with usage and human activities do not show the same affinity. These findings indicate that the locations of the occupation and processing units we sampled are not associated with sites of intensive metal processing or waste disposal (e.g. Cook et al., 2006). Instead, a mechanism of Hg surface enrichment has operated, seemingly alongside the post-occupation development of soils at the site. How enhanced a process this has been and whether the association with human activity at Marco Gonzalez is causal remains to be investigated. It is noteworthy that the topsoil value of Hg in OP13/3 (467.5 ng g⁻¹) is comparable to values (491 ng g⁻¹, $n=30$, range 100-1718) found in London, UK (Yang et al., 2009).

Measurement of Hg and other geochemical variables in surface soil samples at the site is in progress in order to determine whether surface enrichment of Hg is related to proximity to structures, and/or whether other spatial variables such as altitude, soil organic content and vegetation patterns are significant. Similar measurements of geochemical variables in the off-site core sequences are ongoing, to investigate whether or not the timing of enrichment is linked to the occupation or post-occupation periods.

Preliminary analysis of diatom remains found in a core collected from the pool to the south-east of the site, has found that sponge spicules (*Placospongia* sp. and *Chondrosida* sp.) are abundant in deeper carbonate sandy muds, suggestive of reef back-barrier intertidal muds. Diatoms indicative of mudflat/estuarine conditions (e.g. *Navicula peregrina*, *Mastogloia lanceolata*, *Petronis granulata*, *Surirella fastuosa*) are preserved with the transition to fine grain, more organic and non-carbonate muds (contemporaneous with shallowing of the water around the site), while sponge spicules disappear. The robustness of sponge spicules to post-burial dissolution compared to diatom valves may have contributed to the concentrated presence of sponge spicules at the base of the pool sequence but not to their decline further up in the core sample. Their reduction in frequency upwards in the sediment therefore likely relates to a reduction of local sponge habitat due to shallowing (mangrove development) and excessive sedimentation (Bell et al., 2015) during the later occupation of the island. This

finding is important because, as discussed below, clasts of sponge spicule-rich clayey sediment, of presumed local off-site origin, occur as temper within lime plaster floors and as burnt residues in the processing deposits. The same sediment type seems also to be present as intact coatings to Coconut Walk ware sherds (see below).

Bulk soil analyses

Data are presented in online Tables 2-4. *Particle size* analysis proved problematic owing to the large quantities of carbonate present (online Table 3). Only the surface soil from Op 13/3 (Str. 8) and sample x13c at Op 13/2 (Str. 19) stand out as having rather more substantial and coarser carbonate-free sand fractions (~14-16% sand). As natural quartz sand is rare at the site, and often only seen in pottery sherds, any non-calcareous sand concentrations could be regarded as mainly anthropogenic in origin – e.g. pottery disaggregation in surface soils. Soil micromorphology shows that much of the acid-insoluble silt and clay is probably of locally imported non-calcareous fine sediment origin employed as temper fragments in plaster floors and as an industrial raw material in salt working (see below). *LOI* – which reflects a combination of soil organic matter and/or charcoal in the contexts analysed, displays very marked variability (range: 2.02–28.1%). As would be expected, the highest values were recorded in the two topsoil samples, from Structures 8 (*LOI*, 28.1%) and 19 (26.9%). In both these topsoils these high values appear to be attributable to a high soil organic matter content, rather than the presence of large amounts of charcoal, as confirmed by soil micromorphology (see below). Then, this being the case, then it should be noted that these soils are particularly organic-rich, suggesting either that these topsoils have been enriched through anthropogenic activity or that organic decomposition is inhibited by poorly-drained conditions. (In fact, minor waterlogging microfeatures such as plant ferruginisation were noted in thin section, and no artificial additions were in evidence). These surface soil characteristics – as detailed further from the soil micromorphology – is likely linked to the current vegetation cover, and other chemical measurements (Hg, specific conductance, pH, and carbonate content; see Table 1) that help differentiate these soils from ADEs. *Phosphate-P* concentrations are highly variable, with some samples exceptionally enriched, and phosphate being very dominantly inorganic (80->90% inorganic P). At the lower end, 19 samples have concentrations in the range 1.09–4.50 mg g⁻¹; soil micromorphology indicates that these are often layers rich in burnt intertidal sediment fragments. The remaining 20 samples, which have concentrations of 5.42-36.5 mg g⁻¹, are

therefore interpreted as displaying phosphate enrichment to very strong enrichment (online Table 2).

All samples contain high or very high proportions of *carbonate* (range: 33.5–75.0%), with the majority containing $\geq 50.0\%$. All samples analysed also display very marked variability in *specific conductance* ('salinity'). Two of the lowest values were recorded in the two surface soil samples from Structures 8 and 19, with values of 455 and 477 μS , respectively. The values suggest that the upper horizon of the soils is subject to some degree of leaching. The majority of the samples, in contrast, are much more saline ($\geq 2500 \mu\text{S}$), with seven having values $\geq 5000 \mu\text{S}$ (maximum: 5700 μS). Although it seems likely, in this near-coastal environment, that the salts are largely of natural origin (saline groundwater), it should be noted that six of the seven samples with the highest salinity levels contain ash, charcoal and/or burnt residues, and are apparently out of reach of saline ground water. Given these findings, *pH* analyses found that the samples are all alkaline, with expectable pH values ranging from 7.9–9.1. The lowest values were recorded for the two surface soil samples from Structures 8 and 19 (7.9 and 8.0, respectively), which is consistent with their notably lower carbonate content and salinity.

Magnetic susceptibility analyses demonstrated that the χ values are extremely variable, ranging from 4.8–641 $\times 10^{-8} \text{ m}^3 \text{ kg}^{-1}$. Unusually, the χ_{max} values exhibit a similar range (14.8–714 $\times 10^{-8} \text{ m}^3 \text{ kg}^{-1}$) and the resulting χ_{conv} values are exceptionally high ($\geq 37.4\%$), with nine samples having values $\geq 100.0\%$ (i.e. $\chi \geq \chi_{\text{max}}$). These findings are anomalous, but have been encountered before in the study of three tropical African and Mediterranean sites (Crowther, 2014). Thus these data need to be treated with caution. In the specific case of the deposits at Marco Gonzalez where there are burnt ferruginous sediment inclusions, it has been argued that the combined effects of 1) fermentation in exposed tidal mudflats (see below), where enhancement potential could become naturally close to 'saturation', and 2) the burning of such sediments (where they are found as inclusions within lime plaster floors and within the Late Classic processing deposits) may be responsible for these anomalously high values (Graham et al., 2015). In short, the suggested strong effects of fermentation may therefore make indications of heating/burning less evident in both χ and χ_{conv} data. LOI, carbonate, phosphate, specific conductance (salinity) and magnetic susceptibility data are discussed later in relationship to soil micromorphology and context.

4. Soil micromorphology and discussion

Some sixty microstratigraphic layers were described and counted, with one thin section, for example, having 6 units composed of lime plaster floors and use deposits; a number of soil micromorphological descriptions and identifications are complemented by EDS data (online Table 5). The layers are described according to the activities they represent, in chronological order (see Table 1 for summary).

1. Terminal Preclassic (AD 1-250)/Early Classic (AD 250-550/600) settlement activities and island morphology development,
2. Early Classic lime plaster floor constructions (AD 250-550/600),
3. Late Classic intensive processing and associated occupation features (AD 550/600-700/760)
4. A poorly dated Late Classic or possibly later depositional sequence at Op 13-3 (Str. 8) – example of intact weathered lime floor over sands of inundation origin within generally burial and burrow-disturbed stratigraphy.
5. Terminal Classic (AD 760/800-AD 950/1000) to Early Postclassic (AD 1000 to 1250) town, and probable beginning of major deposit weathering and dark earth formation during the less well documented Contact and Colonial Period, with periodic habitation and use until the end of the 16th century and until quite recent times,
6. The modern surface soil and vegetation – the ages of which are unknown although the current vegetation is possibly only of 50-100 years in age .

Terminal Preclassic (AD 1-250)/Early Classic (AD 250-550/600) settlement activities and landscape development

The lowermost sediments—that is, the lowermost accessible deposits before groundwater made sample recovery impossible—as sampled in Op 13-1, Str. 14 (MG 383) (Figs. 3-4) are composed of microlaminated (or burrow homogenised) compact calcitic ash in which there are very abundant small bone inclusions; many inclusions are fish bones, including vertebrae. Notably, in Op 13-2, Str. 19 (MG 391) (Fig. 5), a very similar sediment type is present. At both locations, some bones are pale yellow to almost colourless and are probably poorly preserved ('partly digested/leached') assumed coprolitic bone, whereas orange-coloured and white calcined bones were probably heated and burned, respectively (Macphail and Goldberg 2010). EDS analyses (M4D, MG 383) indicate that coprolitic bones are depleted in Ca and P compared to burnt bone (coprolitic bone: Ca=36.6-37.7%, P=15.6-17.5%; burnt bone: Ca=39.0-39.3%, P=17.1-18.7%; Table 5). The amount of bone overall is consistent with

Contexts MG 383 and MG 391 having some of the highest phosphate concentrations at Marco-Gonzalez (x13b-14d: 22.5-28.1 mg g⁻¹ phosphate-P, *n*=7; Tables 1-2). As two areas of the ashy matrix material were found by EDS to contain 1.99-3.36% P, phosphate in general could have been ‘fixed’ in this calcareous environment, where phosphate is 98.6-99.0% in its inorganic form. It is considered that MG 383 and MG 391 are waterlaid colluvial sediments (Graham et al., 2015).

The presence of waterlaid and now waterlogged sediments is consistent with suggested lower base levels during the initial Maya occupation of the island, with subsequent rise in sea level (Dunn and Mazzullo, 1993) – see Op 13-3 for inundation event. The sediments also record Terminal Preclassic activities which produced large amounts of ash and bone. Such deposits were subsequently eroded, with ensuing colluviation infilling low ground within and around the areas of occupation and into the proximal estuarine/developing mangrove site margins; the last was indicated by Turner’s borehole studies.

At both Op 13-1 (Str. 14) and Op 13-2 (Str, 19) the waterlaid ash sediments were biologically worked, marking a period of exposure and minor weathering (‘soil ripening’). Whereas in Op 13-1 the biologically worked surface was sealed by a series of lime plaster floors (see below—dated to the Early Classic), in Op 13-2, the uppermost biologically worked ashy ‘soils’ record midden remains (uppermost MG 391) sealed by *in situ* ash layers (MG 389; Figs 6-7). Here (MG 389; M13D), there is a 200 mm-thick series of compact ash and trampled occupation floor layers, which continue upwards through M13B (MG 389-386) that are extremely rich in heated and more strongly burnt fish bones that are often horizontally oriented. This amount of bone is consistent with the highest phosphate measurement at the site, for example (x13b – 36.5 mg g⁻¹ phosphate-P). This may be showing renewed occupation associated with processing activity that produced large amounts of fuel ash in the Late Classic Period (MG 389-386; ca. 550-760 AD). (Conjecturally, salt processing deposits raised the occupation surface above water.

At Op 13-1 (Str 14) constructed lime plaster floors (base of MG 382) stratigraphically sealed two cached Early Classic basal-flange bowls (MG 390)(Fig 8). A series of fragmented, but still horizontally oriented lime floors occur alongside their intercalated trampled floor use deposits (Graham et al., 2015). Of particular interest is the use of specific kind of clay clasts as temper within the lime plaster binder. These are isotropic, siliceous in character, and include sponge spicules, and are believed to originate from intertidal/back reef mudflat sediments that are non-calcareous (see Late Classic deposits and plaster floors; EDS online

Table 5: M3A, M3B, M7B). It is conceivable that this addition made the floors stronger; suggested Maya pozzolanic plasters employing volcanic inclusions have been reported from inland Belize (Villaseñor and Graham, 2010).

Late Classic intensive processing and associated occupation features (AD 550/600-700/760)

In Op 13-1, Str. 14, the layers reflecting intensive (salt?) processing were examined from ~2.075-1.070 m asl (MG 359-377) on the east face above the masonry platform (MG 382)(Figs. 4, 10 and 11). On the west face, the same layers (Monolith 7) had subsided into a gap within this rock platform (Monolith 5) so that they extended downwards to 0.530 m asl (MG 377 within MG 382). At Op13-2, Str. 19, this period is represented by deposits between 1.130-0.870 m asl (MG 386 and 389; see Figs 6-7), while mainly only strongly disturbed deposits occur at Op 13-3 (Str. 8) at 0.350-0.170m asl (Figs 5 and 9). A range of layer types can be described, however. As described in Graham et al. (2015), these are:

- a) little disturbed and sometimes totally *in situ* ashy combustion zones,
- b) *in situ* lime plaster floors (Figs 10-11),
- c) chaotically mixed burned sediment clast layers, with various proportions of ash, coarse charcoal and Coconut Walk ware sherds present (Figs 10-11, 12-15), and
- d) trampled occupation surfaces showing minor weathering features and bone-rich kitchen midden waste.

Here, we will only highlight new EDS and microfossil investigations of these facies types.

a) *Totally in situ ashy combustion zones.* These ashy hearth/combustion zone layers, including massive cemented ash and little-weathered ash layers, also display horizontal ash layers thinly interbedded with charcoal (*in situ* hearths). For example, at the base of MG 374, small *in situ* fires with 0.5-1.5 mm-thick ash and charcoal layers are present; it is suggested that these represent fuel layers that were originally ~75-225 mm thick (Courty et al., 1989). One such series of small fires reddened (rubefied) the uppermost 15mm of the 40mm-thick lime plaster floor that capped MG 377 (Figs. 10-11) (see below). Such small fires would have produced low-temperature heating consistent with boiling brine (Biddulph et al., 2012).

b) *In situ lime plaster floors and constructed surfaces* An extensive sequence of lime plaster floors, with trampled occupation soils between the floors, occurs above 1.085 m asl (MG 386; Op 13-1, Str. 14)(Fig 5). A similar sequence begins at a depth of 1.070 m asl (MG 377 to MG 364; Op 13-2, Str. 19) (Figs 10-11). At both locations, the floors include very

large amounts of shell temper, as well as burnt shell of presumed burnt lime origin (EDS data on various inclusions are given in Table 5). As in the Early Classic floors, a major temper component is isotropic clasts of tidal flat sediments rich in siliceous microfossils, such as sponge spicules (M13A: Si=23.4-29.2%; Ca=1.04-1.35%), which occur within the weathered, but often still birefringent, lime plaster matrix (Si=17.3-19.4% Si; Ca=5.06-12.1). As noted above, in Op 13-1, Str. 14, it is clear that there are examples of lime floors/constructed surfaces on which small fires were lit. Detailed EDS studies of the rubefied lime plaster floor surface, its matrix and temper, and an example of Coconut Walk ware were carried out (M3A-B; Table 5; Figs 10-15). It is clear that leaching has affected the surface in M3B, having resulted in lowered interference colours in the uppermost 1-2mm (Ca=4.55-6.52%), whilst laterally and below (3.5-4.00 mm) there has been less decarbonation and decalcification (Ca=6.72-15.0%). Such leaching effects have also probably affected any salt-working residues; no major concentrations of Na and Cl were observed (Na=0.55-1.17%; 0.31-0.67% Cl, n=5). In Op 13-2, Str. 19, however, the sampled floor sequence seems also to record occupation trample between the floors (see below), perhaps indicating domestic or multi-use activities, as indicated in Op 13-1, Str. 14.

c) Chaotically mixed ashy and burned sediment clast layers

At both Structures 14 and 19 there are >1-2m thick layers of pink/rubefied lime plaster floors/constructed surfaces alternating with mixed ash and burnt sediment-rich layers (see Figs. 10-11); small amounts of iron in the isotropic clay clast temper have become rubefied and likely record low temperature (up to 4-500°C) heating as in the Red Hills of Essex (Berna et al., 2007; Biddulph et al., 2012; Dammers and Joergensen, 1996). The deposits forming these layers are alkaline (pH 8.9) and highly saline (specific conductance [μ S] of ~3000-5000), with apparently strongly enhanced high magnetic susceptibility values (see above). On the other hand, the deposits often have relatively low amounts of phosphate (unlike midden occupation floors – see below). In addition to charcoal and ash, their other chief component consists of sediment clasts. The clasts are composed of 1) calcareous and often fossil-rich sediments and 2) much higher quantities (than the calcareous sediments) of isotropic and siliceous microfossil (sponge spicule)-rich sediment materials, which, as suggested above, can be described as non-calcareous tidal flat sediments. EDS on M7B found them to be more Si-rich (Si=19.7-21.7% Si; Ca=1.35-3.04%) compared to calcareous sediment clast types (Si=14.7%;Ca=12.4%) and background ashy ‘fill’ (Si=7.48%; Ca=41.4%). When the siliceous sediment clasts include iron-staining features (Fe=4.47-

4.90%), they are markedly rubefied, which indicates subjection to heat or fire; other burnt iron-stained diatomaceous clay fragments occur within lime plaster floors. The rubefication is indicative of temperatures around 300-400°C (Dammers and Joergensen, 1996), especially as no more strongly altered or vitrified mineral material was found at the site (Berna et al., 2007). The ubiquity of these burnt intertidal sediments is also consistent with the magnetic susceptibility and specific conductance data. As noted previously, the exposure of tidal flat sediments and the resulting concentration of salt are also probably linked to fermentation and a naturally strongly enhanced magnetic susceptibility consistent with a tropical climate; if originally calcareous these may have become decalcified and decarbonated at this time. Why is this burned sediment here, however? As a further consideration, we note that whereas most sherds from the excavations show only a loose coating of background matrix material, two large pottery fragments (quartz sand tempered Coconut Walk ware; M3A Table 5) from processing contexts MG 374 and MG 377, retain isotropic coatings on their interiors (Figs 12-15). The coatings are clearly chemically different from the pot matrix. In addition these are characterised by sponge spicule microfossils and have the same chemistry as the sponge spicule-rich isotropic clay clasts found in these burnt horizons and as lime floor temper (Si=21.3-25.5%; Ca=1.88-7.10%; $n=3$). Given the coring data from the 'pool' (see above) it seems likely that these coatings are formed of siliceous back-barrier mudflat sediment, which suggests an association between the heating of the vessels and the tidal-flat sediments in the putative salt working process.

d) Trampled occupation surfaces showing minor weathering features and bone-rich midden waste. These surfaces were detected in the west face of Op 13-1 and seem to be processing debris (MG 377 within MG 832) that was either dumped, spread, or left exposed owing to a shift in the active processing locale. The deposits here are often compacted and finely fragmented, with horizontal fissuring and horizontally oriented coarse inclusions, which typifies such trampled surfaces (Cammass et al., 1996; Courty et al., 1994). The layers include shell, heated and strongly burnt bone, with much fish bone and some fine amorphous probable coprolitic fragments in places, producing marked phosphate enrichment (x5b: 18.7 mg g⁻¹ phosphate-P; M13A fish bones: P=16.1-17.1%; Ca=37.8-39.0%; F=0.0-2.69%; $n=4$). Intact ash layers are Ca-rich and relatively P-poor (P=0.64%; Ca=62.2%) compared to occupation floors (P=3.72-3.78%; Ca=31.3-34.0%; $n=2$) (Table 5).

Of further note is the occurrence of coarse shell fragments that enclose calcitic, fossiliferous sands of presumed coral beach origin. This suggests that molluscs such as

conchs were processed and then the shells dumped at site peripheries, where coral sand was washed into them; the shells were later collected for various purposes (construction, lime making) and became incorporated in occupation deposits above the beach line.

A poorly dated Late Classic or possibly later depositional sequence at Op 13-3 (Str. 8

Below the dark earth and burial-disturbed upper layers at Op 13-3(see next section), an indurated sandy layer was recorded in the field and a sample was extracted as ‘Ref 2 sand floor’ (Context 385). It is composed of the following layers (Figs 9 and 16-17):

1. 0.42-0.41 m asl: weathered upper lime plaster floor surface,
2. 0.41-0.39 m asl: moderately intact and cemented lime plaster floor which is diffusely microlaminated (‘plastered’), and with tempering composed of much bioclastic (bryozoan) reefstone, and with increased amounts of fine shell and coarse gastropod fragments, downwards; a 10mm-size gastropod (conch?) fragment occurs, at very base of lime floor,
3. 0.39-0.37 m asl: upward-fining (coarse→medium), loose, structureless sand-size carbonate sediment rock fragments, with sand-size reefstone fossils – e.g. bryozoa – shell, including gastropods, and with shell that is often horizontally oriented. Also present is a single 8mm-size pot fragment and few gravel-size clasts.

Archaeological context MG 385 (0.35-0.17 m asl) was assigned to sand that was detected as the highly disturbed deposit (MG 384—mixed charcoal and weathered floor material) was removed. A hard-packed surface of the sandy deposit was then detected, but the MG 385 deposit includes some admixture from beneath the sand layer. Thus the lower part of Context MG 385 as well as MG 387 are charcoal and ash-rich, with a 35mm-thick cemented ash layer found in thin section probably comprising salt working remains. The upper part of MG 385 is distinctive, and made up of upward-fining carbonate sands, which probably record a marine inundation/beach-forming episode of diminishing energy (0.39-0.37 m asl). Both a well preserved (0.39-0.41) and a poorly preserved (0.41-0.42) lime plaster floor overlay the sand. Whatever the event (hurricane-induced sea surge?), the unheated floors overlying the sand could possibly mark a change in use of space from salt processing to domestic ‘town’ occupation during the Late Classic. The amount of sub-floor burials and land crab burrow-mixing material from these two periods makes such an interpretation open to question, however. Of note is that, in the field the floor overlying the sand was unrecognised until soil micromorphology was carried out.

Terminal Classic to Early Postclassic town (AD 760/800-AD 950/1000 to 1250), and Contact and Colonial Period deposit weathering and dark earth formation

Dark earth was studied from Op 13-1, 13-2, 13-3 (Strs. 14, 19, 8), including Context 379 at Op 13/3. Typical of dark earth *sensu lato* (Macphail, 1994; Nicosia et al., In press), there has been weathering and partial to total homogenisation of once stratified archaeological levels, with both decarbonation and decalcifying of *in situ* ‘ghosts’ of lime floors for example in places – yellow brown (YB) deposits noted in the field (Table 5). In areas of large burrows and possible burial pits no *in situ* floor remains occur (Fig. 18). Dark Earth is a mainly blackish, humic and very fine charcoal-rich soil. It can also be coarsely mixed with another microfabric type which is dark yellowish brown because calcareous weathered plaster remains are intimately mixed with charcoal and humus; as would be expected the less Ca-rich dark humic microfabric becomes more dominant upwards (M1A-B; Table 5)(see Figs 19-20). Both soil microfabric types occur as very thin, thin and broad organo-mineral excrements (Bullock et al, 1985), sometimes appearing as loose granules. Residual materials ubiquitously include trace to occasional amounts of burnt and leached coprolitic bone, bryozoan-rich limestone bioclasts (‘reefstone’), (conch?) shell fragments and fine to coarse relict lime floor fragments (Figs 21-22). Root traces and thin shelled gastropods of land snails are also present. Root traces often show weak iron-staining and one unknown root type, which is strongly birefringent (cellulose?) seems to be concentrating Fe (see below)(M1A; Table 5; Figs 19-20). ‘Ghost’ floors often show relict subhorizontal/horizontal concentrations/layers of clay, reefstone and shell tempering that are very weakly cemented by micritic calcite remains.

Bulk soil analyses confirmed the calcareous nature of the Dark Earth (>50% carbonate), but some sample sequences show the progressive effects of leaching up-profile, for example at Op 13/3 (Str. 8), in samples 8c-8a (59.1%→54.8→50.5% carbonate; Table 2). As noted at other sites where carbonate components were high but have been reduced by decarbonation (Duchaufour, 1982)74-75) more strongly residual inclusions and total phosphate can become concentrated (Crowther, 2007; Macphail, 2007). This appears to be the case with the Structure 8 sample 8c-8a sequence (3.66→6.26→7.25 mg g⁻¹ phosphate-P)(Table 2). In Op 13-2 (Str. 19), pH is still alkaline, but leaching seems to have greatly reduced specific conductance some 30cm below the modern surface soil (e.g. as low as 184 μS in sample x12a). Soil micromorphology also shows evident mixing with the modern topsoil at Op 13/3 (Str. 8), and here Hg levels are markedly increased.

Dark earth was also characterised employing SEM/EDS studies at Op 13/1 (Str. 14), on samples M1 (dark earth peds and common but unidentified plant root example) and M1B (dark earth peds above and below lime plaster floor ‘ghost’). These can be summarised as shown in the following (Table 5):

- M1A: Calcareous yellow brown dark earth peds (mesofaunal droppings) formed from weathered anthropogenic layers are more Ca-rich (Ca=30.4-35.3%), compared to less calcareous (decarbonated and partially decalcified) humic dark earth peds (Ca=7.21-20.1%)
- M1A: Iron-stained fibrous root of an unknown plant seems to be concentrating Fe (Fe=9.82-15.1%) compared to background levels in the dark earth soil (Fe=4.45-4.63%).
- M1B: Studies of dark earth over lime floor remains found within the same lime floor, both areas of well-preserved lime plaster (Ca=27.0-27.4%) and decarbonated and decalcified areas (Ca=21.1-22.0%), with Ca in dark earth soil peds varying between 16.0-23.9%, testifying to the differing quantities of finely fragmented carbonate material within the soil.

These data indicate that decarbonisation and decalcification have affected calcareous anthropogenic materials, especially ash and lime plaster. Lime floor ghosts have a lower Ca content compared with ash (62.2-70.4% Ca) and lime floor matrix material (max. 44.4% Ca) from unweathered underlying archaeological layers. The most humic, decarbonated and decalcified dark earth peds appear to be enriched in P, Fe and S, whereas a plant root example is very noticeably rich in Fe, presumably relating to the recycling of Dark Earth soil elements, as detected by XRF analysis of the surface soil. It seems apparent that – ‘Maya Dark Earth’ – owing to the very high carbonate content (reefstone, lime plaster fragments, ash nodules) and relict salt processing residues – is quite different in origin and character when compared to ADE, which have a neutral to acid pH and relatively low Ca content (Arroyo-Kalin, 2010, 2014). In fact, Maya Dark Earth – as a Calcaric Brown Soils *sensu lato* – may have more in common with Roman/post-Roman European Dark Earth formed in the remains of lime-based Roman building materials (plasters and mortars), which have a high base status carbonate-rich character (Macphail, 1994; Nicosia et al., In press). In addition, terms used in European Dark Earth studies might be applicable. For example, ‘pale dark earth’ is used in situations in which weathered building debris dominates and only small amounts of very fine charcoal occur in the matrix soil. ‘Dark Earth’ proper would apply to

situations in which only small amounts of anthropogenic materials remain and the earth is 'dark' owing to the very high concentrations of finely fragmented charcoal that dominate the soil matrix (Macphail and Courty, 1985).

As discussed below, the present-day surface soils – that is, the humic layer – also seem to differ from ADEs. Future studies should include the Maya Dark Earth at Colson Point, Belize, where the geology is non-calcareous (and not reefstone) (Graham, 1994) to test the rigour of the above suggestions.

That land crab action and sub-floor burial have an important role in the formation of Maya Dark Earth is more strongly indicated at Op 13-3 (than at Op 13-1 and Op 13-2) owing to their clear contribution to the homogenization process (compare Figures 4, 5 and 9). Additional studies are essential, however. More needs to be documented concerning the history at the site of crab behaviour (for example, crab burrowing seems to be in evidence in the Terminal Preclassic deposits of Op 13-2 and in the processing deposits at all operations), and more needs to be quantified with respect to the chemical contribution of human burial to the soil. Regarding land crabs, proximity to the ground water table is likely an important factor; thus ground-raising affected the facility with which crabs could reach the water. A further complication was recognised within the dark earth of Op 13-3 (Fig 9), where there was evidence of *in situ* deposition of faecal waste – either of human or possibly pig origin (Macphail and Crowther, 2011; Macphail and Goldberg, 2010). This phenomenon, given where it occurred in the sequence, seems to reflect post-town Late Postclassic or later/colonial occupation(?) and an occurrence contemporary with Dark Earth formation. Dark earth formation cannot, however, simply be dated to the decline of the town in the early 13th century, because the site experienced chronological and spatial variations in use of space in subsequent years. In addition, just as in Roman and Late Roman towns and cities, throughout the site's history there would have been areas of active processing and construction/dwelling, and others where vegetation invaded abandoned house plots, or where plots were used as midden dumps (Macphail, 1994, 2010). As indicated today by Op 13-3, areas at lower elevations would have been prone to flooding and would have been more heavily colonised by land crabs owing to the proximity of the water table.

Modern Litter (L) and surface soil (Ah1 horizon) development

Litter layers (e.g. 20mm-thick) include horizontally oriented leaves and extremely thin organic excrements (of Oribatids?) and broad organic excrements composed of finely comminuted plant fragments (Figs 21-24); aggregated amorphous organic matter produced in

this Litter layer forms broad excrements (granules/crumbs) which embed fine mineral grains and remains of lime floors, shell and reefstone fossils. Faunal remains include land snails. Studies of termite nest reference thin sections suggest that amorphous organic matter probably includes the remains of termite nests. Surface soils are the most organic (highest LOI at 26.9-28.0% LOI) and mercury (Hg)-rich (max 467 ng g⁻¹ Hg), and least alkaline and leached layer type found at Marco Gonzalez (pH=7.9; carbonate=35.9%; specific conductance=455-477 μ S). It is a biologically mixed humic mineral soil and litter (L) layer of a typical broadleaved woodland (see Fig 2) Mull humus horizon type, which is granular to extremely fine pellety in character (Barrat, 1964). Unlike the dark earth, these surface soils and litter layers include very little fine or very fine charcoal and testify to surface accumulation and mixing of organic matter from inputs of plant litter, roots and termite nest materials, and where there has been little anthropogenic disturbance and accretion compared to Maya times. Some secondary iron impregnation features of plant and organic faecal material of mesofauna origin was also noted in thin section, consistent with XRF measurements (Figs 23-24). Although much residual anthropogenic material – fused ash, lime plaster, reefstone, burnt bone, pottery fragments – is present and probably contributes to some strong phosphate concentrations, its formation is in reality related to its current broadleaved caye forest vegetation cover, and thus differs from the underlying dark earth (the exact nature of the vegetation contemporary with Maya occupation and dark earth formation is still a matter speculation, but models of dark earth soil formation in Europe are based on >20 years of monitoring of post-blitz London and Berlin (Macphail, 1994). On the other hand, rooting into the archaeological levels undoubtedly has physically and chemically influenced the development of surface soil and anomalous vegetation cover. How much of an influence is dependent on many factors. For example, Hg concentrations in organic soils are naturally more enhanced from being preferentially adsorbed to organic matter compared to more minerogenic material. Whether Hg has been enriched in the surface soil by root uptake of Hg from depth requires further study, especially owing to plant species-specific differences in uptake and our spatially limited number of excavated samples; it is possible that dietary residues from consumption of large reef fish are a source that is worthy of further investigation. Although roots may contain high concentrations of Hg (reflecting soil Hg), there is often little transportation to above-ground wood and leaves (Greger et al., 2005). If low Hg concentration leaf litter is however permitted to accumulate and degrade (due to high litterfall rates, enhanced microbial activity or sheltered from disturbance) this may provide a

mechanism for Hg enhancement. In addition, these surface soils often have the greatest amount of acid-insoluble quartz sand (~8-14%) compared to the underlying archaeological levels; this could in part be the result of imported quartz sand-tempered pottery breakdown. The study of the present-day surface soil was rewarding in aiding an understanding the weathering and soil formation processes at this Dark Earth site, and future excavations could probably benefit from similar investigations.

5. Discussion and conclusions

The suite of methods was consistent with those used for studying coastal archaeological sites elsewhere. Soil micromorphology (44 thin sections) —entailing SEM/EDS – bulk soil testing for organic matter (LOI), carbonate content, salinity, fractionated phosphate and magnetic susceptibility (39 samples) and particle size analysis from three test pits and surface soils was complemented by XRF elemental analyses and cold vapour-atomic fluorescence spectrometry (CV-AFS) measurements of Hg were carried out on a parallel series of bulk samples. This permitted a fully integrated geochemical investigation. By employing all these findings and background archaeological materials recovery, it has been possible to make both detailed and broad interpretations of the sequences from the three operations (Op 13-1, 13-2 and 13-3; Table 1). In addition, notes on charcoal analysis, the modern vegetation and soil cover, and observations on faunal activity, are included from a multi-author paper (Graham et al., 2015). Although the lower archaeological strata lay below water level, test pits and coring were able to identify ~1 m-thick infilling of low ground with ash and fine bone-rich colluvium in the Terminal Preclassic to Early Classic period (ca. A.D. 1-250). Sediment ripening and lime plaster floors were also found. Major ground raising of at least another metre occurred in Late Classic times (ca. A.D. 550/600 to 700/760), evidenced by alternating ‘pink’ lime floors and charcoal-rich ash layers. In these strata, lime floors – which include burned shell – were rubefied by small fires, now patchily preserved as very thin ash and charcoal layers. These lime ‘floors’, ash, and charcoal layers are believed to be processing remains associated with salt working. Hyposaline salt water from salt pans and/or tidal flat sediments was employed as a brine source (e.g. intact sediment coatings on vessel fragments); the brine was then gently heated over small fires. The salt-processing hypothesis is consistent with the marked presence of rubefied tidal flat sediment clasts in the burned debris layers, which exhibit a high salinity and very strongly enhanced magnetic susceptibility. Weathering effects, including rain and humic acid-associated leaching and

decarbonation, exacerbated by tree root, land crab, and inhumation disturbances which can deeply penetrate the archaeological levels, have developed a specific Maya Dark Earth and modern surface soil type. Reasons why this surface soil at the three sampled profile locations is so mercury-rich are discussed. Only ghosts of lime floors remain in the archaeological levels, and occupational (e.g. burned bone, coprolitic material, conch shell) and processing (burned sediment, fused ash, pottery) debris occur within a dark humic and highly biologically worked soil. Finely fragmented charcoal originating from the Late Classic processing levels greatly contributes to the anomalous colour of the Dark Earth, probably more so than soil humus, *sensu stricto*. In this way, owing to the high carbonate contribution from the carbonate-rich lime-based floors and ash remains, the Marco Gonzalez Dark Earth ('Maya Dark Earth') differs from typical Amazonian Dark Earths. Other sites where weathered lime based building materials have been investigated using soil micromorphology (Straulino et al., 2013) have not had their associated Dark Earth deposits studied in the same way, unfortunately.

Our chief findings can be summarised (Table 1) as:

- Ash and bone-rich colluvium indicates major Terminal Preclassic occupation, although deposits so far investigated are in secondary locations. Intensive marine resource exploitation and coastal trade are indicated by faunal remains and dense sherd deposits.
- Ensuing Early Classic *in situ* occupation deposits include lime plaster floors and interbedded trampled floor deposits, with an example of an extremely bone- and phosphate-rich trampled midden layer. These contexts record the use of isotropic, sponge spicule-rich mud flat clay material as a lime plaster floor temper.
- Heated Late Classic lime plaster floors, ash and *in situ* hearth layers, and dumped highly saline (specific conductance) contexts are dominated by ash and charcoal (fuel waste), burnt sponge spicule-rich mud flat clay clasts. Dumped deposits also contain ceramic sherds, previously implicated in salt processing (Graham 1994: 153-156, Figs. 5.7, 5.8) coated by the same isotropic and sponge-spicule-rich mud flat sediment found as burnt inclusions in the processing deposits. These sherds are from ceramic containers—either bowls or a basin—of a type named 'Coconut Walk unslipped', originally implicated in salt processing at the Colson Point sites along the Belize coast, in the Stann Creek District (Aimers et al. 2015; Graham 1994: 153-156, Figs.

5.7, 5.8). Indications are that salt working at Marco Gonzalez entailed the processing of salt-rich sediments to produce highly concentrated brine (cf. Biddulph et al., 2012). Lime, for plaster floors, seems to have been manufactured by burning shell such as conch. Domestic space was also recorded alongside kitchen middening, weathering and coprolitic inclusions (possible guano); the last may indicate the presence of birds at times, which hints that occupation was seasonal (cf. soil micromorphology of caves such as Mesolithic Uzzo Cave, Sicily; Mannino and Thomas, 2004-6).

- At Op 13-3 (Str. 8), a marine inundation event forming an upward-fining sandy (beach) sediment was recorded above salt working levels, as far as can be judged from this highly disturbed sequence. The natural sands were sealed by an unheated lime plaster floor. Clearly it will be useful to attempt to trace this sand layer outside Op 13-3.
- Deposits that reflect the various construction and occupation activities of people living in the town established at the end of the Classic period and continuing into Terminal and Early Postclassic times did not provide the detail amenable to soil micromorphological study, probably owing to the fact that they were not protected by much in the way of later construction. Skeletal remains of burials of the period, however, and burial accompaniments are generally in good condition. The deposits are broadly characterised as Maya Dark Earth where bio-working and weathering (decalcification and decarbonation) has produced very fine charcoal-rich pellety and granular soils which include weathered ‘ghosts’ of lime plaster floors. These deposits are still calcareous/carbonate-rich owing to the presence of these ‘ghosts’ and large amounts of shell, bioclastic reefstone, and ash nodules, which are relict of hearth deposits and lime floor tempers. Based on present evidence, we suggest that Dark Earth formation was not tied to any specific period in post-Late Classic times, but could have been initiated in any unoccupied space, as suggested in Roman and post-Roman European settlement use of space models.

Modern surface soils are woodland Mull humus horizons with an uppermost leaf litter layer. These differ from the underlying Maya Dark Earth and typical Amazonian Dark Earth, by being humus-rich rather than containing high amounts of very fine charcoal. The surface soils are the result of the current vegetation cover that is recycling nutrients and other elements from the underlying archaeological accumulations, including the Dark Earth. In particular, significantly elevated surface mercury

concentrations adsorbed to organic matter are recorded; mercury could be recycled from dietary residues – large reef fish. The study of the present-day surface soil at Marco Gonzalez has contributed significantly to our understanding of the weathering and soil formation processes at the site. We suggest that the study of modern-day soils should be undertaken more broadly as an excavation strategy because it provides insight into site formation processes. If Dark Earths are investigated because of their fertility, it seems logical to include the modern topsoils formed over them in any investigation, if the full potential of Dark Earths for agricultural sustainability is to be fully appreciated. In addition, the work shows that a further way of understanding how Dark Earth forms and influences the modern soil cover, is through the detailed investigation of topsoils at Maya sites. These are neo-formed through the recycling of nutrients by woodland, forming fertile soils that have been extracted for gardening on the cayes. There are therefore two more areas worthy of investigation identified here.

- 1: Is the Marco Gonzalez Dark Earth unique or common to other Maya sites where lime-based constructions have decayed?, and,
- 2: leading from this, should not modern topsoils be studied alongside these Maya Dark Earths, if the true phenomenon of sustainable agriculture based upon tropical dark earths is to be better understood.

Our intention here is to demonstrate the multi-dimensional significance and expanded potential of soil micromorphological studies. At Marco Gonzalez, such studies have contributed both to our understanding of the character of archaeological deposits (e.g., ghost floors, tidal clasts, working/ walking surfaces reflected in microscopic trampled fish bones, fragmented charcoal, ash clasts and burned sediment). Our knowledge of the cultural significance of such deposits has also been increased, notably by the probable evidence, in the form of tidal flat sediment clasts, of salt processing. Exactly how salt was produced at the site remains to be known, but the tidal flat sediment clasts may reflect the process elucidated by McKillop (2000, 51) in which seawater is poured through salt-saturated sediment to produce an enriched brine for boiling (see also McKillop 2015). At coastal sites excavated by McKillop in southern Belize, evidence has been recovered of brine-boiling jars and their cylindrical supports (2002, 51-52, Fig. 3.1). Similar evidence has not been recovered thus far at Marco Gonzalez, but absence may simply reflect the fact that the processing levels we have encountered contain only the debris of a final stage (McKillop 2002, 51; Reina and

Monaghan 1981), in which salt cakes were produced by heating the enriched brine in the Coconut Walk containers. Our evidence does suggest that the friable vessels were used only once, with the vessel fragments then discarded.

The major drive behind the research focused on Marco Gonzalez, to which knowledge of the Maya cultural dimension is essential, is elucidation of the environmental impact of human activity, particularly the development of the local dark earths. Soil micromorphology has been essential in documenting the history of the deposits at the site—both natural and cultural—after they were laid down. A key finding has been the extent to which depositional elements 'migrate' and can affect surface soils (e.g. the quartz which originates as ceramic temper).

Our research will clearly benefit from more extensive excavation. The Late Classic salt-processing deposits have been exposed only in test pits. The deposits lie beneath the Terminal Classic town's structures with their multitude of burials below house floors, which in turn lie beneath a considerable spread of Postclassic material. The salt processing deposits overlie what appears to be an Early Classic settlement replete with distinctive masonry construction and with evidence of fishing and trading activities that extend back to Terminal Preclassic times. All of this activity is clearly important culturally, perhaps especially in the case of the burst of salt production that parallels Late Classic florescence on the mainland. From our point of view, however, the association of the site with Dark Earth formation provides an example in which intensive human activity can be associated with enhanced soil fertility. There is no evidence thus far from our research that intentionality was involved in dark earth formation (Graham et al. 2015), although further archaeological investigation is essential to clarify the activities represented by the charcoal layers. Nonetheless the association tells us that even inadvertent human behaviour--living, working, discarding, leaving debris, dying--can potentially affect soils positively, and this outcome has implications today both for long-term estimates of soil fertility and the decision-making involved in the contents of land fill and the future of land fill sites.

6.Acknowledgments

We thank Dr. John Morris and the staff of the Institute of Archaeology, National Institute of Culture and History, for granting permission to carry out the work in Belize. The multi-disciplinary undertaking in 2013 and 2014 that produced the research reported here would not have been possible without funding provided through a Research Grant from the Leverhulme

Trust. Additional funding has been provided by the UCL Institute of Archaeology and the UCL Institute for Sustainable Research. Excavations at Marco Gonzalez in 1986 and 1990 were funded by the Social Sciences and Humanities Research Council of Canada and the Royal Ontario Museum. Graham thanks her co-PI, Scott Simmons, for kindly tolerating her divergence into soils research. We thank David Pendergast for his continued support and advice on our project and its publications, and are indebted to Jan Brown, Chairman of the Board of the Marco Gonzalez Maya Site, Ambergris Caye, Ltd., Preservation Group for all her efforts on our behalf. We thank Eduardo Barrientos and Denver Cayetano from the University of Belize and Dr. Elma Kaye, Terrestrial Science Director of the Environmental Research Institute, for their invaluable assistance, and Jerry Choco for excellent site management. Macphail gratefully acknowledges Tom Gregory and Kevin Reeves (Institute of Archaeology, University College London) for their SEM/EDS support. For supporting the ideas over the years that led to the field research, Graham would like to thank William Woods, William Balée, Eduardo Neves, Dirse Kearns, Paul Sinclair, Tim Beach, Sheryl Luzzader-Beach, and the Royal Botanic Garden Edinburgh, especially Peter Furley, Sam Bridgewater and David Harris.

7. References

- Aimers, J., Haussner, E., Farthing, D., 2015. The ugly duckling: insights into ancient Maya commerce and industry from pottery petrography. In: Morris, J., Badillo, M., Batty, S., Thompson, G. (Eds.), 89-95. Institute of Archaeology, National Institute of Culture and History (NICH), Belmopan, Belize.
- Aimers, J., Haussner, E., Farthing, D., Murata, S., 2016/In press. An Expedient Pottery Technology and Its Implications for Ancient Maya Trade and Interaction. In: Walker, D. (Ed), Perspectives on the Ancient Maya of Chetumal Bay. University Press of Florida, Gainesville.
- Arroyo-Kalin, M., 2009. Steps towards an ecology of landscape: the pedo-stratigraphy of anthropogenic dark earths. In: Woods, W.I., Teixeira, W., Lehmann, J., Steiner, C., WinklerPrins, A., Rebellato, L., (Eds.), Amazonian Dark Earths: Wim Sombroek's Vision. Springer Science, New York/Berlin, pp. 99-125.
- Arroyo-Kalin, M., 2010. The Amazonian Formative: Crop Domestication and Anthropogenic Soils. *Diversity* 2, 473-504.
- Arroyo-Kalin, M., 2014. Amazonian Dark Earths: geoarchaeology. In: Encyclopedia of Global Archaeology, Volume 1, Springer, New York, pp. 168-178.

-
- Arroyo-Kalin, M., Neves, E. G., and Woods, W. I., 2008. Anthropogenic Dark Earths of the Central Amazon Region: Remarks on their evolution and polygenetic composition. In: Woods, W. I., Teixeira, W. G., Lehmann, J., Steiner, C., WinklerPrins, A. M. G. A., Rebellato, L. (Eds.), *Amazonian Dark Earths: Wim Sombroek's Vision*. Springer Science, New York/Berlin, pp. 99-125.
- Avery, B. W., Bascomb, C. L., 1974. *Soil Survey Laboratory Techniques*. Harpenden, Soil Survey of England and Wales, Soil Survey Technical Monograph.
- Ball, D. F., 1964. Loss-on-ignition as an estimate of organic matter and organic carbon in non-calcareous soils. *Journal of Soil Science*, 15, 84-92.
- Barrat, B. C., 1964. A classification of humus forms and microfabrics in temperate grasslands. *Journal of Soil Science*, 15, 342-356.
- Beach, T., Dunning, N., Luzzadder-Beach, S., Cook, D. E., Lohse, J., 2006. Impacts of the ancient Maya on soils and soil erosion in the central Maya Lowlands. *Catena*, 65, 2, 166-178.
- Beach, T., Dunning, N. P., 1995. Ancient Maya terracing and modern conservation in the Peten rain forest of Guatemala. *Journal of Soil and Water Conservation*, 50, 138-145.
- Beach, T., Terry, R., Brown, C., Luzzadder-Beach, S., 2009. Terra Preta in Maya soils. Paper Presented at the Association of American Geographers Annual meeting, Las Vegas NV, 26 March.
- Bell, J., McGrath, E., Biggerstaff, A., Bates, T., Bennett, H., Marlow, J., Shaffer, M., 2015. Sediment impacts on marine sponges. *Marine Pollution Bulletin*, 94, 1-2, 5-13.
- Berna, F., Behar, A., Shahack-Gross, R., Berg, J., Boaretto, E., Gilboa, A., Sharon, I., Shalev, S., Shilstein, S., Yahalom-Mack, N., Zorn, J. R., Weiner, S., 2007. Sediments exposed to high temperatures: reconstructing pyrotechnological processes in Late Bronze Age and Iron Age Strata at Tel Dor (Israel). *Journal of Archaeological Science*, 34, 358-373.
- Biddulph, E., Foreman, S., Stafford, E., Stansbie, D., Nicholson, R., 2012. *London Gateway. Iron Age and Roman salt making in the Thames Estuary; Excavations at Stanford Wharf Nature Reserve, Essex*. Oxford, Oxford Archaeology.
- Boorman, L., Hazelden, J., Boorman, M., 2002. New salt marshes for old - salt marsh creation and management. In: *Littoral 2002, The Changing Coast*. Porto - Portugal, EUCC, pp. 35-45.

-
- Borderie, Q., Devos, Y., Nicosia, C., Cammas, C., Macphail, R. I., 2014, Chapter 18. Dark Earth in the geoarchaeological approach to urban contexts. In: Arnaud-Fassetta, G., and Carcaud, N. (Eds.), *French geoarchaeology in the 21st century*. Paris, CNRS, pp. 245-258.
- Bullock, P., Fedoroff, N., Jongerius, A., Stoops, G., Tursina, T., 1985. *Handbook for Soil Thin Section Description*. Waine Research Publications, Wolverhampton.
- Cammass, C., Wattez, J., Courty, M.-A., 1996. L'enregistrement sédimentaire des modes d'occupation de l'espace. In: Castelletti, L., Cremaschi, M. (Eds.), *Paleoecology; Colloquium 3 of XIII International Congress of Prehistoric and Protohistoric Sciences, Volume 3*. ABACO, Forli, pp. 81-86.
- Cook, D. E., Kovacevich, B., Beach, T., Bishop, R., 2006. Deciphering the inorganic chemical record of ancient human activity using ICP-MS: a reconnaissance study of late Classic soil floors at Cancuen, Guatemala. *Journal of Archaeological Science*, 33, 5, 628-640.
- Courty, M. A., 2001. Microfacies analysis assisting archaeological stratigraphy. In: P. Goldberg, Holliday, V. T., Ferring, C. R. (Eds.), *Earth Sciences and Archaeology*. Kluwer, New York, 205-239.
- Courty, M. A., Goldberg, P., Macphail, R. I., 1989. *Soils and Micromorphology in Archaeology*. Cambridge University Press, Cambridge.
- Courty, M. A., Goldberg, P., Macphail, R. I., 1994. Ancient people - lifestyles and cultural patterns. In: Etchevers, J. D. (Ed.), *Transactions of the 15th World Congress of Soil Science, International Society of Soil Science, Mexico, Volume 6a*. International Society of Soil Science, Acapulco, pp. 250-269.
- Crowther, J., 2007. Chemical and magnetic properties of soils and pit fills. In: Whittle, A. (Ed), *The Early Neolithic on the Great Hungarian Plain: investigations of the Körös culture site of Ecsefalva 23, Co. Békés., Volume I*. Institute of Archaeology, Budapest, pp. 227-254.
- Crowther, J., 2014. Chemistry, magnetic susceptibility and particle size of various contexts from the Marco Gonzalez Maya site, Belize. In: Graham, E. (Ed.), *The Investigations at Marco Gonzalez, 2013-14, Report submitted to the Belize Institute of Archaeology, Belmopan, Belize*. Institute of Archaeology, University College London, London.
- Dammers, K., Joergensen, R. G., 1996. Progressive loss of Carbon and Nitrogen from simulated daub on heating. *Journal of Archaeological Science*, 23, 639-648.

-
- Dick, W. A., Tabatabai, M. A., 1977. An alkaline oxidation method for the determination of total phosphorus in soils. *Journal of the Soil Science Society of America*, 41, 511-514.
- Duchaufour, P., 1982. *Pedology*. Allen and Unwin, London.
- Dunn, R. K., Mazzullo, S. J., 1993. Holocene paleocoastal reconstruction and its relationship to Marco Gonzalez, Ambergris Caye, Belize. *Journal of Field Archaeology* 20, 2, 121-131.
- Gischler, E., Hudson, H. J., 2004. Holocene development of the Belize Barrier Reef. *Sedimentary Geology*, 164, 223-236.
- Gischler, E., Lomando, A. J., Hudson, J. H., Holmes, C. W., 2000. Last interglacial reef growth beneath Belize barrier and isolated platform reefs. *Geology*, 28, 387-390.
- Glanville-Wallis, F., 2015. 'Of Crabs and Men': Artefact analysis of residual waste deposits and a preliminary investigation into crab bioturbation at Marco Gonzalez, Belize [BSc Archaeology Dissertation]. London, Institute of Archaeology, University College London.
- Glaser, B., Birk, J.J., 2012. State of the scientific knowledge on properties and genesis of Anthropogenic Dark Earths in Central Amazonia (terra preta de índio). *Geochimica et Cosmochimica Acta* 82, 39-51.
- Glaser, B., Woods, W.I. (Eds.), 2004. *Amazonian Dark Earths: Explorations in Space and Time*. Springer-Verlag, Berlin.
- Goldberg, P., Macphail, R. I., 2006 *Practical and Theoretical Geoarchaeology*. Blackwell Publishing, Oxford.
- Graham, E., 1994. *The Highlands of the Lowlands: Environment and archaeology in the Stann Creek District, Belize, Central America*. Monographs in World Archaeology 19. Prehistory Press, Madison, Wisconsin and Royal Ontario Museum, Toronto.
- Graham, E., 1998. Metaphor and metamorphism: some thoughts on environmental meta-history. In: Balée, W., (Ed.), *Advances in Historical Ecology*. Columbia University Press, New York, pp. 119-137.
- Graham, E., 2006. A Neotropical Framework for *Terra Preta*. In: Balée, W., Erickson, C. L. (Eds.), *Time and Complexity in Historical Ecology*. Columbia University Press, New York, pp. 57-86.
- Graham, E., Pendergast, D. M., 1989. Excavations at the Marco Gonzalez Site, Ambergris Cay, Belize, 1986. *Journal of Field Archaeology*, 16, 1-16.

-
- Graham, E., Pendergast, D. M. 1992. Maya urbanism and ecological change. In: Steen, H. K., Tucker, R. P., (Eds), *Changing Tropical Forests*. Forest History Society/Duke University Press, Durham, N.C., pp. 102-109.
- Graham, E., Simmons, S. R. 2012. Ambergris Caye, Belmopan. Report on the 2010 Excavations at Marco Gonzalez, Ambergris Caye (Submitted to the Belize Institute of Archaeology, Belmopan). Institute of Archaeology, University College London, London.
- Graham, E., Macphail, R. I., Turner, S., Crowther, J., Stegemann, J., Arroyo-Kalin, M., Duncan, L., Whittet, R., Rosique, C., Austin, P. 2015. The Marco Gonzalez Maya site, Ambergris Caye, Belize: Assessing the impact of human activities by examining diachronic processes at the local scale. *Quaternary International* xxx, pp. 1-28.
<http://dx.doi.org/10.1016/j.quaint.2015.08.079>
- Greger, M., Wang, Y., Neuschütz, C., 2005. Absence of Hg transpiration by shoot after Hg uptake by roots of six terrestrial plant species. *Environmental Pollution*, 134, 2, 201-208.
- Heiri, O., Lotter, A. F., Lemcke, G., 2001. Loss on ignition as a method for estimating organic and carbonate content in sediments: reproducibility and comparability of results. *Journal of Paleolimnology*, 25, 101-110.
- James, N. P., Ginsburg, R. N., 1979. *The Seaward Margin of Belize Barrier and Atoll Reefs*. Special Publication No. 3, International Association of Sedimentologists. Blackwell Scientific, Oxford.
- Lehmann, J., Kern, D.C., Glaser, B., Woods, W.I. (Eds.), 2003. *Amazonian Dark Earths: Origin, Properties, Management*. Kluwer Academic, Dordrecht, Netherlands.
- Macphail, R. I., 1994. The reworking of urban stratigraphy by human and natural processes. In: Hall, A. R., Kenward, H. K. (Eds), *Urban-Rural Connexions: Perspectives from environmental Archaeology*, Monograph 47. Oxbow, Oxford, pp. 13-43.
- Macphail, R. I., 2003. Soil microstratigraphy: a micromorphological and chemical approach. In: Cowan, C. (Ed.), *Urban development in north-west Roman Southwark Excavations 1974-90*, Monograph 16. MoLAS, London, pp. 89-105.
- Macphail, R. I., 2007. Soil micromorphology (Chapter 11). In: Whittle, A., Kovács, G. (Eds.), *The Early Neolithic on the Great Hungarian Plain: investigations of the Körös culture site of Ecsegfalva 23, Co. Békés*. Institute of Archaeology, Budapest, pp. 189-226.

-
- Macphail, R. I., 2010, Dark earth and insights into changing land use of urban areas, *in* Speed, G., and Sami, D., eds., *Debating Urbanism: Within and Beyond the Walls c. AD 300 to c. AD 700* (Conference Proceedings Leicester University Nov 15th 2008), Volume Leicester Archaeology Monograph 17: Leicester, Leicester Archaeology, p. 145-165.
- Macphail, R. I., Allen, M. J., Crowther, J., Cruise, G. M., Whittaker, J. E., 2010. Marine inundation: effects on archaeological features, materials, sediments and soils. *Quaternary International*, 214, 44-55.
- Macphail, R. I., Courty, M. A., 1985. Interpretation and significance of urban deposits. In: Edgren, T., Jungner, H. (Eds.), *Proceedings of the Third Nordic Conference on the Application of Scientific Methods in Archaeology*. The Finnish Antiquarian Society, Helsinki, pp. 71-83.
- Macphail, R. I., Crowther, J., 2011. Experimental pig husbandry: soil studies from West Stow Anglo-Saxon Village, Suffolk, UK. *Antiquity Project Gallery*, Volume 85, 330, *Antiquity* (<http://antiquity.ac.uk/projgall/macphail330/>).
- Macphail, R. I., Crowther, J., Berna, F., 2012. Soil micromorphology, microchemistry, chemistry, magnetic susceptibility and FTIR. In: Biddulph, E., Foreman, S., Stafford, E., Stansbie, D., Nicholson, R. (Eds.), *London Gateway. Iron Age and Roman salt making in the Thames Estuary; Excavations at Stanford Wharf Nature Reserve, Essex* (<http://library.thehumanjourney.net/909>), Oxford Archaeology Monograph No. 18, Oxford Archaeology, Oxford.
- Macphail, R. I., Cruise, G. M., 2001. The soil micromorphologist as team player: a multianalytical approach to the study of European microstratigraphy. In: Goldberg, P., Holliday, V., Ferring, R. (Eds.), *Earth Science and Archaeology*. Kluwer Academic/Plenum Publishers, New York, pp. 241-267.
- Macphail, R. I., Goldberg, P., 2010. Archaeological materials. In: Stoops, G., Marcelino, V., Mees, F. (Eds.), *Interpretation of Micromorphological Features of Soils and Regoliths*. Elsevier, Amsterdam, pp. 589-622.
- Mannino, M. A., Thomas, K., 2004-6. New radiocarbon dates for hunter gatherers and early farmers in Sicily. *Accordia Research Papers*, 10, 13-33.
- McKillop, H., 2002. *White Gold of the Ancient Maya*. University Press of Florida, Gainesville.

-
- McKillop, H., 2015. Evaluating ancient Maya salt production and the domestic economy: the Paynes Creek salt works and beyond. In: Morris, J., Badillo, M., Batty, S., Thompson, G., pp. 97-105. Institute of Archaeology, National Institute of Culture and History (NICH), Belmopan, Belize.
- Nicosia, C., Devos, Y., Macphail, R. I., In press. European 'Dark Earth'. In: Nicosia, C., Stoops, G. (Eds.), *Encyclopedia of Archaeological Soil and Sediment Micromorphology*. Blackwell, Oxford.
- Pendergast, D. M., Graham, E., 1987. No site too small: the ROM's Marco Gonzalez excavations in Belize. *Rotunda*, 20, 1, 34-40.
- Reina, R.E., Monaghan, J., 1981. The ways of the Maya: salt production in Sacapulas, Guatemala. *Expedition* 23: 13-33.
- Schiffer, M. B., 1987. *Formation Processes in the Archaeological Record*. University of New Mexico Press, Albuquerque,.
- Scollar, I., Tabbagh, A., Hesse, A., Herzog, I., 1990. *Archaeological prospecting and remote sensing*. Cambridge University Press, Cambridge.
- Sombroek, W. G., 1966, *Amazon Soils. A Reconnaissance of the Soils of the Brazilian Amazon Region*. Centre for Agricultural Publication and Documentation, Wageningen.
- Stoops, G., 2003. *Guidelines for Analysis and Description of Soil and Regolith Thin Sections*. Soil Science Society of America, Inc., Madison, Wisconsin.
- Stoops, G., Marcelino, V., Mees, F., 2010. *Interpretation of Micromorphological Features of Soils and Regoliths*. Elsevier, Amsterdam.
- Tite, M. S., 1972. The influence of geology on the magnetic susceptibility of soils on archaeological sites. *Archaeometry*, 14, 229-236.
- Tite, M. S., Mullins, C. E., 1971. Enhancement of magnetic susceptibility of soils on archaeological sites. *Archaeometry*, 13, 209-219.
- Villaseñor, I., Graham, E., 2010. The use of volcanic materials for the manufacture of pozzolanic plasters in the Maya lowlands: a preliminary report. *Journal of Archaeological Science*, 37, 1339–1347.
- Weiner, S., 2010. *Microarchaeology. Beyond the Visible Archaeological Record*. Cambridge University Press, Cambridge.
- Woods, W.I., Teixeira, W., Lehmann, J., Steiner, C., WinklerPrins, A., Rebellato, L. (Eds.), 2009. *Amazonian Dark Earths: Wim Sombroek's Vision*. Springer, London.

Yang, H., Berry, A., Rose, N. L., Berg, T., 2009. Decline in atmospheric mercury deposition in London. *Journal of Environmental Monitoring*, 11, 1518-1522.

Table 1: Details of samples analysed; Structures (Str) 8 (Op 13/3), 14 (Op 13/1) and 19 (Op 13/2)

Bulk sample	Thin section	Notes from field and thin section studies
x0-5cm Str8		Surface soil
x8a	M8A	Homogeneous black humic with very abundant roots; sand-size flecks of sand/cemented ash/lime floor fragments – Dark Earth
x8b	M8B	Homogeneous black humic with very abundant roots; sand-size flecks of sand/cemented ash/lime floor – Dark Earth and weathered lime plaster floors
x8c	M8C	Greyish brown - brown, finely fragmented ash, with few to many roots (coarse shell example) – Dark Earth and broad burrow
xMRef3	MRef3	Context 376 – weathered but intact lime plaster floor
x9a	M9A	Blackish semi-homogenised with sharp junctions with cemented layers, rooted – Dark earth and weathered lime plaster floors
x9b	M9B	Burrow and root channel mixed blackish and brownish yellow processing/ash residues with rubefied fragments – Dark earth-lime plaster floors
x9c	M9C	Burrow and root channel mixed blackish and brownish yellow processing/ash residues with rubefied fragments – ash residue layer
xMRef2	MRef2	Weathered, but intact lime plaster floor over calcareous beach sand (marine flooding)
x10a	M10A	Burrowed processing ash waste and lime floor fragments over cemented ash layer
x10b	M10B	Fragmented cemented ash processing waste, lime floor, embedded charcoal and pot
x1a Str 14	M1A	Homogenised rooted soil – Dark Earth
x1b	M1C	Burnt marine sediment fragments (salt working)
x2a	M2A	Strongly biomixed mixed plaster and salt-working remains and humic Dark Earth
x2b	M2B	Bioworked decalcified plaster floors and integrated very fine charcoal; Dark Earth
x2c	M2D	Rubefied, burned layer; burrowed lime floor and salt working debris
x2d	M2D	Charcoal lens; ash and charcoal-rich debris dump, with trampled occupation surface
x3a	M3A	Mixed charcoal and pinkish 'ash' residues; charcoal debris and lime floor fragments
x3b	M3B	Pinkish residues, burned mineral inclusions; lime plaster floors and thin in situ hearths
x3c	M3C	Rubefied lime floor surface – in situ hearth
x3d	M3C	Brownish mineral layer - laminated ash over bone-rich kitchen midden
x3e	M3D	Weathered plaster floor surface
x3f	M3C-M3D	Semi-homogenised sands, burned min and charcoal - fine pot frags at top - weathering horizon; includes trampled occupation and salt working debris layers
x5a	M5A	Brownish with charcoal; burnt sediments from salt working

Bulk sample	Thin section	Notes from field and thin section studies
x5b	M5A	Homogenous grey – trample; rich in heated fishbone, guano(?) and coprolitic bone
x5c	M5B	Grey with charcoal and 'ash'; fuel ash and burnt sediments – salt processing debris
x6a	M6	Intact sample - whitish deposit; originally colluvial ashy kitchen waste-rich sediment
x4a rock platform	M4A	Very dark grey layer; ashy and lime floor fragment-rich occupation dump?
x4b	M4D	Greyish brown layer; waterlaid colluvial bone-rich ash, with included latrine waste
x0-5cm Str 19	M11	Surface soil; mixed litter (L) and totally biologically-worked Ah1 organo-mineral horizon
x12a	M12A	Brown, humic, strongly biologically-worked ash and lime plaster floor residues
x12b	M12B	Blackish and dark brownish, 'indurated' layer; humic-stained intact lime floor
x13a	M13A	Series of layered reddish brown ash residues (~3cm thick; x13a) and thin charcoal layers (~0.5cm thick); occupation trample and lime floors
x13b	M13C	Rather pure ash layer; kitchen midden with very high burnt bone content
x13c	M13D	Dark grey over grey, weathered ash-rich layer; soil formed in colluvial ash
x14a	M14A	Dark greyish, homogeneous; rooted, partially biologically worked colluvial ash
x14b	M14B	Whitish grey; laminated waterlaid ashy colluvium rich in fine bone; footslope location?
x14c	M14C	Mixed pale and dark grey and charcoal - horizontal pot frag; burrowed plaster floors
x14d	M14D	Mixed pale and dark grey; burrowed ashy colluvium containing bone and coprolites

Table 2: LOI, carbonate, pH, conductance, phosphate-P, magnetic susceptibility and Hg (mercury) data

Bulk sample	LOI ^a (%)	Carbonate ^b (CaCO ₃ equiv, %)	pH ^c	Specific conductance ^d (μ S)	Phosphate- P ^e (mg g ⁻¹)	χ^f (10 ⁻⁸ m ³ kg ⁻¹)	χ_{max}^f (10 ⁻⁸ m ³ kg ⁻¹)	χ_{conv}^f (%)	Hg ^g (ng g ⁻¹)
x0-5cm Str8	28.1***	35.1	7.9	455	11.4**	70.3	188	37.4	467.5
x8a	12.0**	50.5*	8.6*	1900*	7.25*	87.3	167	52.3	204.6
x8b	8.67*	54.8*	8.7*	2220*	6.26*	88.1	157	56.1	189.6
x8c	6.24*	59.1*	8.8*	2240*	3.66	127*	145	87.6	82.2
xMRef3	4.41	58.8*	9.1*	1090*	2.32	212*	225	94.2	53.4
x9a	5.41*	57.9*	8.9*	2620**	4.50	139*	158	88.0	128.8
x9b	5.36*	59.3*	8.7*	2880**	2.42	209*	209	100	54.2
x9c	5.34*	60.9*	8.6*	4080**	1.88	206*	191	>100	27.3
xMRef2	2.02	75.0**	9.0*	2340*	1.15	59.4	57.3	>100	29.6
x10a	5.24*	57.6*	nd	nd	1.82	203*	197	>100	74.9
x10b	3.28	61.7*	nd	nd	1.92	164*	155	>100	36.2
x1a Str. 14	7.22*	52.1*	8.9*	697	5.42*	197*	214	92.1	213.5
x1b	6.51*	43.4	8.8*	1420*	2.00 [†]	444*	440	>100	44.3
x2a	2.61	60.1*	nd	nd	3.12 [†]	77.8	92.3	84.3	32.8
x2b	12.6**	47.7	8.7*	2500**	2.00 [†]	144*	166	86.7	64.3
x2c	8.12*	44.0	8.7*	2930**	3.65 [†]	362*	348	>100	38.9
x2d	18.4**	45.4	nd	nd	1.62	105*	144	72.9	34.5
x3a	19.9**	49.7	8.5*	5260***	1.09	163*	244	66.8	31.6
x3b	5.89*	33.5	8.7*	5220***	2.10 [†]	641*	714	89.8	40.1
x3c	14.4**	56.0*	8.6*	5700***	1.19 [†]	110*	198	55.6	26.1
x3d	7.28*	53.0*	8.8*	4900**	6.67*	257*	303	84.8	50.6
x3e	3.72	63.8*	8.8*	3340**	1.37	96.4	189	51.0	44.1
x3f	6.99*	48.6	8.8*	5070***	5.66*	374*	402	93.0	42.9
x5a	5.39*	48.9	8.9*	5010***	5.52*	286*	323	88.5	63.5
x5b	5.84*	54.9*	8.9*	3980**	18.7**	85.4	159	53.7	48.8
x5c	9.21*	55.1*	nd	nd	5.43* [†]	158*	205	77.1	37.6

Bulk sample	LOI ^a (%)	Carbonate ^b (CaCO ₃ equiv, %)	pH ^c	Specific conductance ^d (μ S)	Phosphate- P ^e (mg g ⁻¹)	χ^f (10 ⁻⁸ m ³ kg ⁻¹)	χ_{max}^f (10 ⁻⁸ m ³ kg ⁻¹)	χ_{conv}^f (%)	Hg ^g (ng g ⁻¹)
x6a	4.65	65.8*	nd	nd	21.2***	4.8			34.6
x4a	5.51*	60.5*	8.7*	5580***	22.5***	121*	111	>100	56.4
x4b	3.66	70.2*	8.9*	3540**	23.2***	8.6	14.8	58.1	40.0
x0-5cmStr19	26.9***	39.4	8.0	477	8.09*	120*	194	61.9	241.4
x12a	5.42*	58.3*	8.4	184	3.91	86.2	137	62.9	104.1
x12b	8.65*	50.0*	nd	nd	3.26 [†]	132*	175	75.4	75.7
x13a	5.87*	48.0	8.5*	5020***	7.03*	388*	451	86.0	28.6
x13b	2.70	59.4*	8.8*	3620**	36.5***	17.8	16.3	>100	14.6
x13c	4.02	58.8*	8.7*	3560**	25.3***	76.3	99.4	76.8	45.7
x14a	3.85	56.6*	nd	nd	26.9***	62.4	81.3	76.8	50.4
x14b	3.91	63.4*	8.8*	3680**	22.4***	16.5	21.0	78.6	29.7
x14c	3.30	67.1*	8.8*	3040**	24.5***	16.1	26.8	60.1	43.5
x14d	3.36	65.0*	8.8*	3480**	28.1***	13.1	20.4	64.2	47.5

^a **LOI:** values highlighted indicate notably higher LOI values, which reflects the amount of organic matter and/or charcoal present: * = 5.00–9.99%, ** = 10.0–19.9%, *** \geq 20.0%.

^b **Carbonate:** values highlighted indicate higher carbonate concentrations: * = 50.0–74.9%, ** \geq 75.0%.

^c **pH:** values highlighted indicate pH \geq 8.5; nd = not determined because of insufficient sample.

^d **Specific conductance:** values highlighted indicate higher values: * = 1000–2440 μ S, ** = 2500–4990 μ S, *** \geq 5000 μ S; nd = not determined because of insufficient sample.

^e **Phosphate-P:** [†] indicates that phosphate-P was determined on residual samples from the LOI analysis (see footnote of Table 3); values highlighted indicate likely phosphate-P enrichment: * = ‘enriched’ (5.00–9.99 mg g⁻¹), ** = ‘strongly enriched’ (10.0–19.9 mg g⁻¹), *** = ‘very strongly enriched’ (20.0–39.9 mg g⁻¹).

^f **Magnetic susceptibility:** data are difficult to interpret (see text and Graham *et al.*, Forthcoming); χ values \geq 100 x 10⁻⁸ m³ kg⁻¹ are highlighted.

^g **Mercury (Hg):** CV-AFS data suggest particular enrichment of surface and near-surface Dark Earth layers

For Hg measurements a 0.2g subsample of the milled sediment was digested in aqua regia for 2h at 100°C in rigorously acid-leached 50 ml polypropylene digestion tubes. Digested solutions were analysed for Hg using cold vapour-atomic fluorescence spectrometry (CV-AFS) following reduction with SnCl₂. Standards and quality control blanks were measured with the sample run to monitor measurement stability. Reference stream sediment GBW07305 (certified Hg value 100 ng g⁻¹) digested with the samples gave 103 ng g⁻¹, RSD = 3.2 ng g⁻¹ (n=3).

Table 3: Particle size analysis of carbonate-free, peroxide-treated soil

Bulk sample	Coarse sand 600 μm – 2.0 mm (%)	Medium sand 200-600 μm (%)	Fine sand 60-200 μm (%)	Silt + clay ^a <60 μm (%)
x0-5cm Str8	3.3	4.6	5.7	86.4
x1a	2.0	2.7	3.5	91.8
x1b	0.2	0.5	1.6	97.7
x2c	0.2	0.4	1.4	98.0
x3d	0.6	1.1	2.8	95.6
x3f	1.1	2.7	4.2	92.0
x0-5cm Str19	0.9	3.0	3.7	92.4
x13c	4.7	6.6	4.9	83.8
x4a Str 14	0.0	0.7	1.4	97.9
x4b	1.0	2.5	3.0	93.6

^a As detailed in the text, particle size analysis proved problematic in that the clay fraction did not fully disperse.

Table 4: Phosphate fractionation data

Bulk sample	Phosphate- P _i (mg g ⁻¹)	Phosphate- P _o (mg g ⁻¹)	Phosphate- P (mg g ⁻¹)	Phosphate- P _i :P (%)	Phosphate- P _o :P (%)
x0-5cm	9.87	1.56	11.4	86.4	13.6
x8a	5.82	1.43	7.25	80.3	19.7
x8b	5.35	0.914	6.26	85.4	14.6
x8c	3.14	0.524	3.66	85.7	14.3
xMRef3	2.05	0.271	2.32	88.3	11.7
x9a	4.23	0.274	4.50	93.9	6.1
x9b	2.15	0.272	2.42	88.8	11.2
x9c	1.64	0.243	1.88	87.1	12.9
xMRef2	1.10	0.052	1.15	95.5	4.5
x10a	1.55	0.272	1.82	85.1	14.9
x10b	1.76	0.159	1.92	91.7	8.3
x1a	5.00	0.421	5.42	92.2	7.8
x1b	1.77	0.233	2.00	88.4	11.6
x2a	2.97	0.147	3.12	95.3	4.7
x2b	nd	nd	2.00	nd	nd
x2c	nd	nd	3.65	nd	nd
x2d	nd	nd	1.62	nd	nd
x3a	nd	nd	1.09	nd	nd
x3b	1.74	0.360	2.10	82.9	17.1
x3c	nd	nd	1.19	nd	nd
x3d	nd	nd	6.67	nd	nd
x3e	1.28	0.087	1.37	93.6	6.4
x3f	5.17	0.491	5.66	91.3	8.7
x5a	5.14	0.378	5.52	93.1	6.9
x5b	18.1	0.635	18.7	96.6	3.4
x5c	nd	nd	5.43	nd	nd
x6a	20.9	0.306	21.2	98.6	1.4
x4a	21.8	0.715	22.5	96.8	3.2
x4b	22.8	0.351	23.2	98.5	1.5
x0-5cm	6.85	1.24	8.09	84.7	15.3
x12a	3.60	0.314	3.91	92.0	8.0
x12b	nd	nd	3.26	nd	nd
x13a	6.47	0.556	7.03	92.1	7.9
x13b	36.1	0.362	36.5	99.0	1.0
x13c	24.8	0.537	25.3	97.9	2.1
x14a	26.3	0.580	26.9	97.8	2.2
x14b	22.1	0.298	22.4	98.7	1.3
x14c	24.2	0.325	24.5	98.7	1.3
x14d	27.7	0.399	28.1	98.6	1.4

nd = Not determined because of
discolouration (from organic matter and/or
charcoal) in acid extracts; in these cases
phosphate-P was determined on residual
samples from the LOI analysis

Table 5: Marco Gonzalez SEM/EDS area analyses; M1A, M1B, M3A, M3B, M4D, M7B and M13A (selected microfeatures and elements %)

Feature	Na	Mg	Al	Si	P	S	Cl
<i>M1A (Op 13/1, Str.14, Layer 359)</i>							
<i>Dark earth soil A</i>							
Unidentified plant root (n=3)	2.50-7.45	4.76-11.1	11.0-13.6	4.05-7.28			0.0-5.86
Soil infill in root		11.1	9.02	12.2	0.74		0.39
Local dark earth soil		9.03	7.96	11.3		0.47	
<i>Dark earth soil B</i>							
Yellow-brown thin and broad peds with calc. anthrop. Residues (n=3)	0.0-0.52	7.27-8.19	6.04-8.30	9.12-10.0	0.65-0.77	0.0-0.36	0.0-0.29
Thin ped; poorly calc. humic soil	0.37	10.9	7.76	22.1	1.04	0.22	
Thin ped; humic soil	0.79	6.94	9.54	13.5	1.46	0.54	
<i>M1B (Op 13/1, Str.14, Layer 359)</i>							
<i>Dark earth – lime floor sequence</i>							
<i>Overlying dark earth soil</i>							
Residual lime floor fragment	0.34	9.89	8.74	13.6	0.69	0.34	0.22
Dark earth soil peds (n=2)	0.50-0.63	8.93-10.7	8.50-9.14	11.8-13.0	0.71-0.87	0.0-0.33	0.0-0.26
Bryozoan bioclast	0.42						
Soil peds immediately above floor	0.36	10.6	8.60	16.8	0.55	0.37	0.42
<i>Weathered lime floor layer</i>							
Calclitic lime floor layer (n=2)	0.34-0.42	8.97-9.56	7.18-7.49	12.0-13.2	0.0-0.53	0.29-0.34	0.31-0.35
Weathered floor layers (n=2)	0.0-0.43	11.1-11.9	7.66-8.23	12.2-14.2	0.63-0.84	0.31-0.52	0.43-0.68
<i>Lime floor inclusions</i>							
Burned non-calcareous pot	4.99	1.62	9.65	27.3		0.38	0.67
Quartz grain within pot fragment		0.20	0.39	45.8			
Bryozoan bioclast (reefstone)		6.29	0.24			0.47	
<i>M3A Op 13/1(Str. 14, Layer 374)</i>							
<i>Coconut Walk Pot</i>							
Matrix	1.38	1.54	11.5	29.5			0.19

Quartz sand temper	0.11	0.01	0.09	46.5 (99.4%Si O ₂)			0.06
Background calcareous deposit	0.70	5.99	4.61	7.23		0.31	0.25
Pot coating (n=3)	1.62-1.89	7.43- 10.3	10.4-11.5	21.3- 24.5	0.24-0.42	0.09- 0.22	0.71- 1.07
M3B Op 13/1(Str. 14, Layer 374)							
<i>Rubefied lime plaster floor area A</i>							
Leached rubefied surface 0-3.5mm (n=2)	0.65-0.75	13.0- 14.1	11.3-11.5	14.4- 16.5	0.47-0.65	0.0- 0.35	0.36- 0.67
Ditto – 1mm depth	1.17	12.1	13.3	16.2	0.50	0.44	0.51
Ditto – 2mm depth	0.65	12.9	13.9	16.5	0.51	0.24	0.48
Rubefied lime plaster floor 3.5-4mm; residual lime plaster	0.55	13.1	10.5	13.6	0.34	0.17	0.31
<i>Rubefied lime plaster floor area B; leached surface</i>							
Isotropic clay (with sponge spicules) temper	0.61	8.70	11.0	25.1	0.21		0.53
Lime matrix-isotropic clay temper boundary (n=3)	0.75-0.87	11.3- 12.6	12.4-14.4	16.6- 19.7	0.29-0.52		0.36- 0.47
M7B (Str. 14, Layer 377)							
<i>Burnt 'clay' deposit A</i>							
Burnt clay clast 1 (isotropic, sponge spicules)(n=2)	0.0-0.82	9.00- 11.3	9.68-9.81	19.7- 20.7			1.01- 1.52
Calcareous/ashy 'fill'		5.03	3.89	7.48			0.69
Non-calcareous matrix 'fill'		10.4	14.9	13.6			2.43
<i>Burnt 'clay' deposit B</i>							
Burnt clay clast 2 (isotropic, sponge spicules)	1.45	8.75	12.8	21.7			0.65
Poorly-calcareous 'fill'		9.17	9.26	17.1			1.57
Shell			0.43				
Calcareous sediment clast (fine shelly)		10.0	9.42	14.7			


<i>M13A Op 13-2(Str. 19, Layer 359)</i>							
<i>Trampled floors</i>							
Crushed heated fish bone? (n=2)	0.84-1.00	1.22-1.30	0.25-0.38		16.1-16.8	0.63-0.67	1.13-1.26
Occupation floor deposit (upper)	0.52	5.50	3.72	11.9	2.22	0.32	0.35
Occupation floor deposit (lower)		4.95	3.78	14.9	2.25		0.58
Compact ash layer (micritic calcite)		5.15	0.64		0.43	0.52	
<i>Loose layered deposits</i>							
Heated serrated fishbone? (n=2)	0.75-1.08	1.28-1.36	0.0-0.31		16.2-17.1	0.40-0.63	0.58-1.19
Coarse (wood?) ash (n=2)		0.88-1.14					
Wood charcoal	4.36	14.4	6.05	1.96			2.60
<i>Lime plaster floor</i>							
Burnt isotropic clay temper (sponge spicules)(n=2)	1.47-1.51	5.95-6.66	13.1-13.3	23.4-23.9	0.0-0.30		0.99-1.24
Lime plaster floor matrix	0.88	11.0	9.98	17.3			1.40
<i>(Conch?) shell fragment</i>							
shell	0.73		0.58				
Weathered shell		2.56	0.94			0.54	
<i>Weathered lime floor</i>							
Bryozoan bioclast		7.03	0.26			0.58	
Isotropic sediment inclusion	0.63	7.74	8.63	29.2	0.24		1.01
Weathered lime floor	0.65	10.3	12.4	19.4	0.45		0.81
<i>M4D Op 13-1 (Str. 14, Layer 383)</i>							
Coprolitic fish vertebrae (n=3)	0.84-1.02	1.34-1.75	0.21-1.78	0.0-0.41	15.6-17.5	0.49-0.72	0.42-0.64
Vertebra: calcitic void infill		3.21		1.27	8.56		
Matrix sediment	0.59	3.74	1.05	1.19	3.36		0.38
Small fish bone section area (n=2)	1.05-1.06	0.88-1.42	0.0-0.97	0.0-0.35	16.0-18.7	0.41-0.43	0.54-0.62
Lime floor fragment	0.63	2.08	0.56		0.64	0.19	0.45
Ditto – weathered halo	0.82	2.61	0.73	1.20	1.51	0.19	0.29
Orange and calcined (burnt) fish bone (n=2)	0.47-1.13	0.29-1.31	0.15-0.39		17.1-18.7	0.0-0.43	0.26-0.45

Table 6: Summary of soil micromorphology and bulk soil findings

Contexts/Structures	Soil micromorphology and bulk soil data interpretations	Period and further information
<p>Surface soil Litter (L) and Ah1 horizon Op 13/2-3 (Str.19 and 8) and Structure 25</p>	<p>Most organic (highest LOI) and mercury (Hg)-rich, and least alkaline layer, with biologically mixed humic mineral soil and litter (L) layer of typical Mull humus horizon, which is granular to extremely fine pelley in character. Elevated mercury, adsorbed to organic matter, is believed to be due to surface soil accumulation from the underlying anthropogenic deposits – drawing on natural marine Hg accumulators - large reef fish – plus potential use of the element during Maya occupation. Relatively high phosphate levels may result from relict bone and possible effects of decomposition of inhumations (also likely influencing character of dark earth). Litter includes horizontally oriented leaves and extremely thin organic excrements (of Oribatids?) and broad organic excrements composed of finely comminuted plant fragments; aggregated amorphous organic matter produced in this Litter layer forms broad excrements (granules/crums) which embed fine mineral grains and remains of lime floors, shell etc. Fauna include land snails and amorphous organic matter is probably part remains of termite nests (which have also contributed to reference thin sections).</p> <p>Unlike the dark earth, these surface soils and litter layers include very little fine or very fine charcoal and testify to surface accumulation and mixing of organic from inputs of plant litter, roots and termite nest materials. The plants at the site have recycled chemicals including mercury, iron and probably phosphate into the organic matter from the underlying anthropogenic deposits. In addition, as carbonate-rich residual materials were decalcified, phosphate-rich material – bone, cess etc – would have been relatively concentrated, while plant humus accumulation concentrated mercury.</p>	<p><i>Modern</i> Vegetation survey (R. Whittet and C. Rosique in Graham et al., Forthcoming) found that the mangrove-surrounded island has an interestingly rich flora (64 species) with a wooded central part broadly consistent with “Caye Forest” and “Caye Broadleaved Forest” classifications, with salt-tolerant plants on its margins and some few patches of recently introduced species (e.g. <i>Cocos</i>).</p> <p>Topsoil measurements also found elevated concentrations of Hg across the island (S. Turner in Graham et al., Forthcoming)</p> <p>Land crab activity/burrowing at lower elevations (Glanville-Wallis, 2015); hermit crab use of ancient conch shells.</p>
<p>Dark earth Op 13/1-3 (Str. 14, 19 and 8)</p>	<p>Typified by total biological microfabrics of very fine charcoal-rich soil – hence dark colour – containing relict clasts of resistant burned sediment, ash nodules and calcined bone, for example, while lime plaster floors and</p>	<p>Town established in Late Classic to Terminal Classic times (late 8th to early 9th century) and occupied into</p>

<p>Op 13/3 (Str. 8) Context 379</p>	<p>fragments show dissolution and sometimes recrystallization of calcite (micrite), and can occur as ‘ghost’ layers. Leaching has caused marked reduction specific conductance (salinity) and progressive decrease in carbonate content; phosphate however can increase up-profile. Also Hg-rich when burrow-mixed with humic surface soils.</p> <p>Essentially recemented ghost of lime plaster floor(s) within ‘dark earth’ and showing calcitic root pseudomorphs of weathering history. Upwards there are only finely fragmented gravel size floor remains, with a marked modern total biological microfabric, and increased humic content (LOI) and phosphate in a broad burrow/feature fill (grave?) that is also modern rooted. Upwards (Contexts 366 and 376) relict and fragmented lime plaster floor soil is increasingly mixed with more humic and very fine charcoal rich soil – including humic peds worked down from modern topsoil. Within this dark earth, however, there was <i>in situ</i> deposition of faecal waste – either of human or possibly pig origin, recording post-town Late Postclassic and later/colonial occupation(?).</p>	<p>the Early Postclassic (ca. AD 1200); structures of this period are characterised by numerous sub-floor burials. Less intensive use of the site after the Early Postclassic but residential and ritual activity continues through to the Contact period (1500s). The town was built over stratified salt processing debris that dates to the Late Classic (ca AD 600 to 750). Land crabs are active throughout these periods but apparently where the water table is more easily accessible, i.e. at low elevations.</p>
<p>Op 13/3 (Str. 8) Context 380</p> <p>Context 384</p> <p>Context Upper 385</p>	<p>Weathered and biologically burrowed soil formed in lime plaster floor remains, with semi-intact layers present; minor increased amounts of organic matter and slightly less carbonate are consistent with nearer surface weathering, while increased phosphate may be of ‘town’ character; upwards, more humic and totally biologically worked dark earth soil. Diffusely and broadly layered ~10-15mm thick remains of decalcified lime floor and moderately intact lime floor remains (burnt shell remains suggest continued use of burnt shell as a lime source); less evidence of use of tidal flat clays as temper/addition compared to salt processing levels and earlier. Domestic lime floor over marine sands (marine inundation high point at 0.37 m asl).</p>	<p>No primary dating from this structure; estimated from ceramics to date from the Late/Terminal Classic to Early Postclassic (see above). Sub-floor burials present but heavily disturbed; extensive disturbance by land crabs has mixed Late Classic salt processing (AD 600-750) with later floors associated with Str. 8.</p>
<p>Op 13/1 (Str. 14) Contexts 359-377 and Structure 19 Context 386</p>	<p>Salt working deposits formed of mainly layered:</p> <ol style="list-style-type: none"> little disturbed and sometimes totally <i>in situ</i> ashy combustion zones, <i>in situ</i> lime plaster floors, chaotically mixed burned marine sediment clast layers (with high specific conductance and magnetic susceptibility), with various proportions 	<p>Late Classic salt processing (AD 550/600 to 700/760) High concentrations of crudely made, roughly standardised quartz sand-tempered pottery vessels</p>

<p>Op 13/3 (Str. 8) Context 385</p> <p>Context 387</p>	<p>of ash and coarse charcoal present, and d) occasional trampled occupation surfaces showing minor weathering features and bone-rich kitchen midden waste; presence of shells which had ‘trapped’ fossiliferous beach sands.</p> <p>Findings suggest use of tidal flat sediments (probably ‘upper salt marsh’ environment) for source of concentrated salt, which when mixed with sea water produce a strong brine; this was heated on small low temperature fires located on lime plaster floors which acted as the hearth base. Mainly siliceous fossil (sponge spicule)-rich fine tidal flat sediment was employed – as also found coating quartz sand-tempered Coconut Walk pot fragments. Some mollusc shells, once processed for food, and which were discarded on the beach, were sometimes recycled for constructions or lime burning.</p> <p>15-20mm-thick lime floor (with decalcified weathered upper surface), constructed on medium to coarse and fine to medium upward-fining beach sands at 0.39m asl. This indicates Late Classic marine inundation event (storm surge?). End of Late Classic salt-processing and post-inundation development of Late Classic-Terminal Classic town at 0.39m asl.</p> <p>Burrowed and finely fragmented remains of weakly rubefied lime plaster floors, burned clay, ash and charcoal; loose fine charcoal coats plaster and ash clasts; 35mm-thick intact partially ‘cemented’ ash layer survives within burrowed zone. (Addition of siliceous clay to lime plaster floors, may, like Roman concrete be added to produce neoformed aluminium silicates – and specially hard and water-proof plasters).</p>	<p>(Coconut Walk ware) for holding brine and fuel waste wood charcoal of species?? occur; quartz sand not local to island (Graham et al., forthcoming).</p> <p>(Probable crab burrows)</p>
<p>Op 13/1 (Str.14) Context 382</p> <p>Op 13/2 (Str. 19) Contexts 389-386</p>	<p>Construction of a series of lime plaster floors (for example over a cached Early Classic bowl), tempered with isotropic siliceous microfossil (sponge spicule)-rich tidal flat sediment clasts of various sizes (silt to gravel size), and incorporating charcoal and fine burned bone, with pure micritic lime plastered surfaces, conceivably of ash(?) origin.</p> <p>Upwards, 391 is sealed by a series of ash layers (389-386) – some ‘wetted’ and recemented – with an interbedded series of thin trampled deposits, which can be extremely rich in heated/burned bone (mainly fish bone) and for example record the highest phosphate content at Marco-Gonzalez. In</p>	<p>Early Classic occupation (AD 250 to 550/600)</p> <p>Macrofossils of maize (<i>Zea mays</i>) and craboo (<i>Byrsonima</i> sp.) is indicative of trade (L. Duncan in Graham <i>et al.</i>, Forthcoming).</p>

	 <p>this 'domestic' occupation area, these are presumed fireplaces used for food preparation which may have included low temperature cooking/smoking of fish.</p>	
<p>Op 13/1 (Str. 14) Context 383 and Op 13/2 (Str. 19) Context 391 (389?)</p>	<p>Rainstorm erosion of putative ash-rich hearths, with associated burned bone (cooking), heated bone (low temperature cooking - food processing – smoking?) and human waste (coprolitic bone), all including fish bone, producing waterlaid ashy sediments in low ground. High energy colluviation resulted in coarse lens composed of gravel-size lime plaster, pot, bone, bioclastic limestone and charcoal. Exposure and short period of stasis led to weak weathering effects and biological working of the uppermost sediments at both locations. At Structure 19 these were composed of shell- and bone-rich kitchen midden deposits at the top of Context 391. Anthropogenic nature of waterlaid sediments implies high occupation concentrations upslope.</p>	<p>Protoclassic to Terminal Preclassic occupation (ca. AD 100-250?) Coring data suggests the presence of such 'early' ash-rich sediments on the now-mangrove covered margins of the island (see S. Turner in Graham et al., forthcoming). Macrofossils of maize (<i>Zea mays</i>) and craboo (<i>Byrsonima</i> sp.) is indicative of trade (L. Duncan in Graham <i>et al.</i>, Forthcoming).</p>

Figs

Fig 1: Regional location map? – need higher resolution image please.

Fig 2: Aerial photo of MG showing wooded area within mangrove

Fig. 3: MG – location of structures 8 (Op 13-3), 14 (Op 13-1) and 19 (Op 13-2) – need higher resolution image please.

Fig. 4: Field photo of labelled Op 13-1 (Str 14) – need higher resolution image please.

Fig. 5: Field photo of labelled Op 13-2 (Str 19) – need higher resolution image please.

Fig. 6: Thin section scan – M13D – 391 and 386 junction – Early Classic – Late Classic?

Fig. 7: Photomicrograph M13D – details of bone-rich ashy, middening soil and overlying in situ ash. PPL – Early Classic – Late Classic?

Fig. 8: Cached pot sealed by plaster floors - need higher resolution image please.

Fig. 9: Field photo of labelled Op 13-3 (Str 8)

Fig. 10: TS scan of M3B – heated lime floor with overlying fuel ash waste, etc (sediment-coated coconut walk pot also in pic) EDS studies on pot and plaster floor

Fig. 11: TS scan of M7A – other side of sondage – same material;

Fig. 12: Photomicrograph of coated pot PPL

Fig. 13: Ditto – OIL

Fig. 14: Detail PPL

Fig. 15: Pot – coating SEM image and Spectrum location

Fig. 16: MG – Ref 2 – lime floor over upward-fining calc fossiliferous sands

Fig. 17: Ditto – photomicrograph of junction OIL.

Fig. 18: Scan of M2A – lime floor frags in DE.

Fig. 19: Photomicrograph of M1A – section through EDS-studied plant root – within pelley DE, XPL 4.62mm

Fig. 20: Ditto at 2.38mm PPL

Fig. 21: Photomicrograph of M1A – floor frag in DE soil – PPL

Fig. 22: Ditto – OIL.

Fig. 23: Scan of MG14-M2 surface soil with Litter layer

Fig. 24: Photomicrograph of MG14-M2 surface soil – leaf litter – 4.62mm PPL

Fig. 25: Ditto – detail at 0.90mm – very thin pelley organic excrements – PPL

Fig. 26: Ditto OIL – showing iron staining

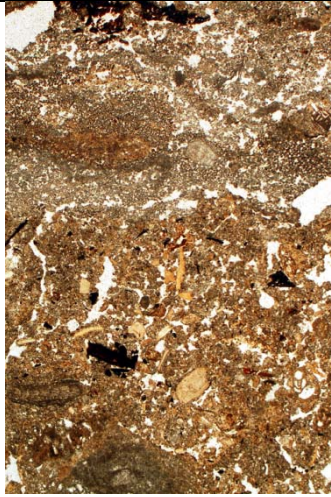


Fig 7 – to be labelled



Fig 8



Fig 9 – to be labelled



Fig 10 – to be labelled



Fig 11 – to be labelled

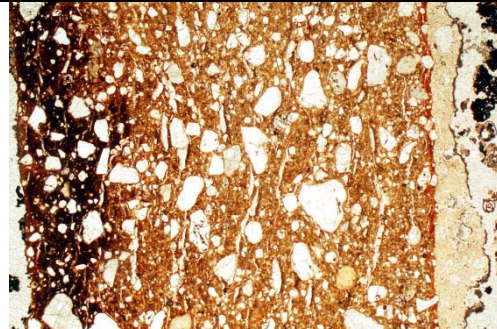


Fig 12 – to be labelled

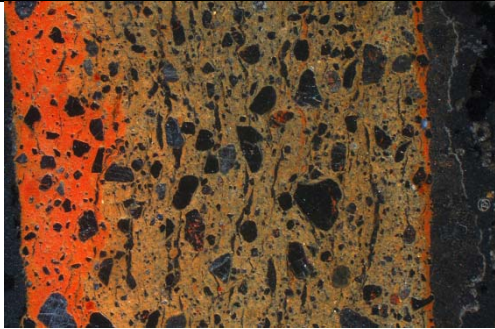


Fig 13 – to be labelled

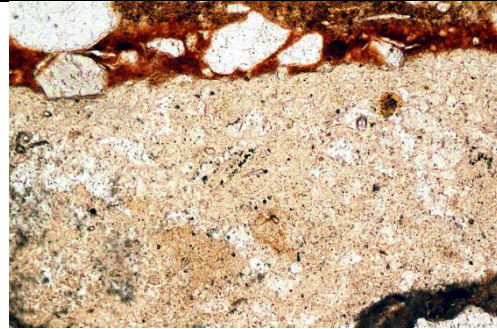


Fig 14 – to be labelled

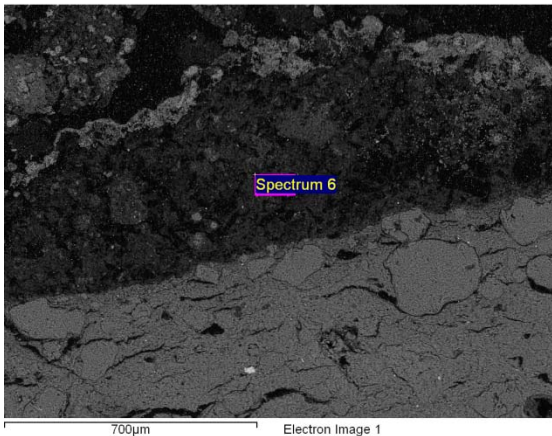


Fig 15 – to be labelled



Fig 16 – to be labelled

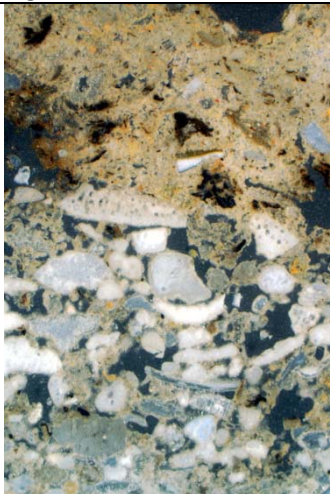


Fig 17 – to be labelled



Fig 18 – to be labelled



Fig 19

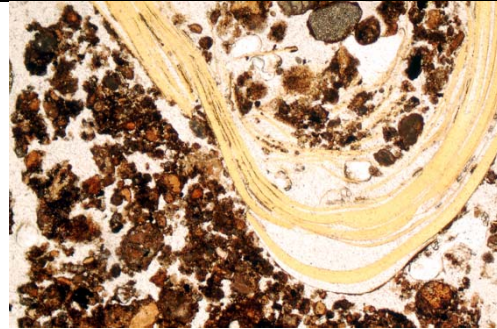


Fig 20

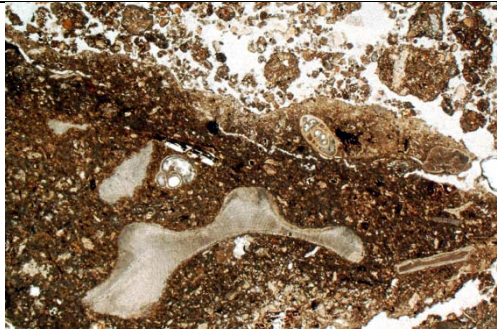


Fig 21 – to be labelled

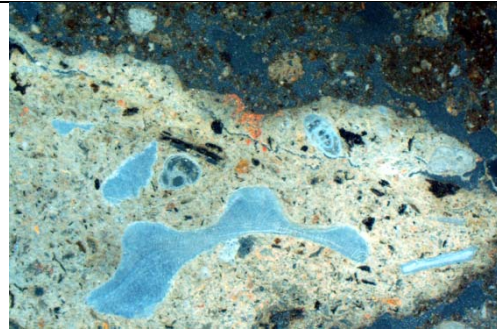


Fig 22 – to be labelled



Fig 23 – to be labelled

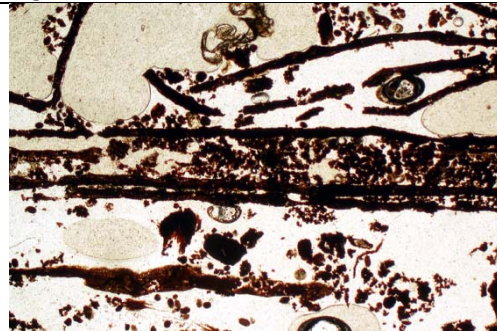


Fig 24 – to be labelled

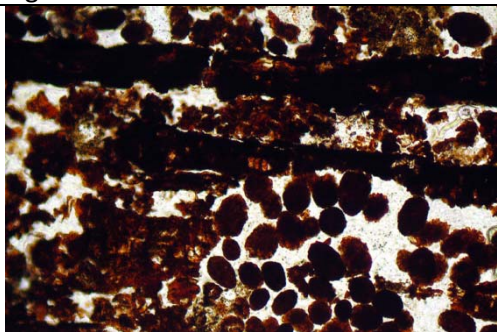


Fig 25

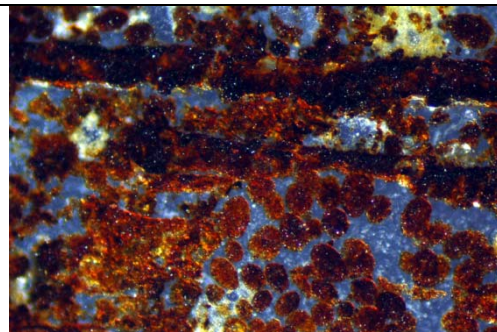


Fig 26